



UNIVERSITY OF LEEDS

This is a repository copy of *Controls on fluvial sedimentary architecture and sediment-fill state in salt-walled mini-basins: Triassic Moenkopi Formation, Salt Anticline Region, SE Utah, USA*.

White Rose Research Online URL for this paper:  
<http://eprints.whiterose.ac.uk/80265/>

Version: Accepted Version

---

**Article:**

Banham, SG and Mountney, NP (2013) Controls on fluvial sedimentary architecture and sediment-fill state in salt-walled mini-basins: Triassic Moenkopi Formation, Salt Anticline Region, SE Utah, USA. *Basin Research*, 25 (6). 709 - 737. ISSN 0950-091X

<https://doi.org/10.1111/bre.12022>

---

**Reuse**

Unless indicated otherwise, fulltext items are protected by copyright with all rights reserved. The copyright exception in section 29 of the Copyright, Designs and Patents Act 1988 allows the making of a single copy solely for the purpose of non-commercial research or private study within the limits of fair dealing. The publisher or other rights-holder may allow further reproduction and re-use of this version - refer to the White Rose Research Online record for this item. Where records identify the publisher as the copyright holder, users can verify any specific terms of use on the publisher's website.

**Takedown**

If you consider content in White Rose Research Online to be in breach of UK law, please notify us by emailing [eprints@whiterose.ac.uk](mailto:eprints@whiterose.ac.uk) including the URL of the record and the reason for the withdrawal request.



[eprints@whiterose.ac.uk](mailto:eprints@whiterose.ac.uk)  
<https://eprints.whiterose.ac.uk/>

# **Controls on fluvial sedimentary architecture and sediment-fill state in salt-walled mini-basins: Triassic Moenkopi Formation, Salt Anticline Region, SE Utah, USA**

Steven G. Banham<sup>1</sup> and Nigel P. Mountney<sup>1</sup>

*1 – Fluvial & Eolian Research Group, School of Earth and Environment, University of Leeds, Leeds, LS2 9JT, UK.*

## **Abstract**

The Triassic Moenkopi Formation in the Salt Anticline Region, SE Utah represents the preserved record of a low-relief ephemeral fluvial system that accumulated in a series of actively subsiding salt-walled mini-basins. Development and evolution of the fluvial system and its resultant preserved architecture was controlled by: (i) the inherited state of the basin geometry at the time of commencement of sedimentation; (ii) the rate of sediment delivery to the developing basins; (iii) the orientation of fluvial pathways relative to the salt walls that bounded the basins; (iv) spatially and temporally variable rates and styles of mini-basin subsidence and associated salt-wall uplift, and (iv) temporal changes in regional climate. Detailed outcrop-based tectono-stratigraphic analyses demonstrate how three coevally developing mini-basins and their intervening salt walls evolved in response to progressive sediment loading of a succession of Pennsylvanian salt (the Paradox Formation) by the younger Moenkopi Formation, deposits of which record a dryland fluvial system in which flow was primarily directed parallel to a series of elongate salt walls. In some mini-basins, fluvial channel elements are stacked vertically within and along the central basin axes, in response to preferential salt withdrawal and resulting subsidence. In other basins, rim synclines have developed adjacent to bounding salt walls and these served as loci for accumulation of stacked fluvial channel complexes. Neighbouring mini-basins exhibit different styles of infill at equivalent stratigraphic levels: sand-poor basins dominated by fine-grained, sheet-like sandstone fluvial elements, which are representative of non-channelised flow processes, apparently developed synchronously with neighbouring sand-prone basins dominated by

major fluvial channel-belts, demonstrating effective partitioning of sediment route-ways by surface topography generated by uplifting salt walls. Reworked gypsum clasts present in parts of the stratigraphy demonstrate the subaerial exposure of some salt walls, and their partial erosion and reworking into the fill of adjoining mini-basins during accumulation of the Moenkopi Formation. Complex spatial changes in preserved stratigraphic thickness of four members in the Moenkopi Formation, both within and between mini-basins, demonstrates a complex relationship between the location and timing of subsidence and the infill of the generated accommodation by fluvial processes.

Keywords: salt; fluvial; halokinesis; Moenkopi Formation; Triassic; Paradox Basin; tectono-stratigraphy

### ***Introduction***

Globally, there exist in excess of 120 provinces where the action of salt tectonics has governed basin formation and influenced the style of sediment infill (Hudec & Jackson, 2007). Documented examples record the development of both passive and reactive salt structures associated with either extension or compression, and the development of structures related to differential loading and flexural buckling of overburden (Vendeville & Jackson, 1992a, b; Jackson *et al.*, 1994, Waltham, 1997). The initiation of salt mobilisation and the onset of salt-related mini-basin development due to subsurface salt withdrawal into adjacent salt walls is triggered by a variety of factors, including buoyancy, differential loading (Ge *et al.*, 1997), thermal convection, and the presence of extensional or contractional tectonic regimes (Jackson & Talbot, 1986; Waltham, 1997; Hudec *et al.*, 2009; Ings & Beaumont, 2010; Fuchs *et al.*, 2011).

The growth and evolution of salt walls in the subsurface can result in a variety of surface topographic expressions, the form of which is dependent on: (i) the rates and styles of mini-basin subsidence and associated salt-wall uplift, which combine to generate accommodation; and (ii) the rate of sedimentation that serves to fill accommodation. Topographic surface expressions arising from the growth of salt-structures at depth can assume a variety of forms,

including subtle swells, ridges and walls, each of which act to deform overlying strata to generate surface expression, and piercement structures where the deforming salt itself breaches the surface (Trusheim, 1960; Ala, 1974; Jackson & Talbot 1986; Jackson *et al.*, 1990; Davison *et al.*, 1996a; Lawton & Buck, 2006). The architecture and location of salt structures at depth are commonly controlled by pre-existing basement structures such as inherited fault arrays, whereby salt-wall development tends to be triggered above or immediately adjacent to points of differential salt thickness (Cater, 1970; Smith *et al.*, 1993; Doelling, 2002a). Evolving salt-walls and adjacent mini-basins therefore develop with a range of planform geometries and surface expressions including parallel, elongate linear ridges such as those present in the Salt Anticline Region of SE Utah (Harrison 1927; Dane, 1935; Trudgill 2011) and the South Urals mini-basins (Newell *et al.*, 2012), or complex interacting polygonal patterns such as those of the Triassic of the Central North Sea (Smith *et al.*, 1993; Stewart, 2007) and the Permo-Triassic Pre-Caspian Basin of Kazakhstan (Barde *et al.*, 2002; Volozh *et al.*, 2003).

Once salt movement has been initiated, mini-basin subsidence due to salt withdrawal into adjacent, growing salt walls is enhanced by the effects of sediment loading as active depositional systems accumulate strata in evolving mini-basin depocentres (Jackson & Talbot, 1986; Hudec *et al.*, 2009), a process referred to as downbuilding (Barton, 1933). Once initiated, salt-walled mini-basins tend to evolve rapidly with documented subsidence rates up to 10 km.Ma<sup>-1</sup> (Prather, 2009) allowing thick accumulations of strata to be preserved over relatively short episodes of geologic time. Where salt-wall growth generates a surface topographic expression, it dictates processes of sedimentation and styles of accumulation of sedimentary architecture by controlling surface sedimentary processes, including sediment distribution route-ways, and by controlling complex spatial and temporal trends in the rate of creation of accommodation.

Examples of currently active halokinesis include the Zagros Mountain Belt and Qum Kuh of Iran (Ala, 1974; Talbot, 1998; Talbot & Aftabi, 2004), the Gulf of Mexico (Wu *et al.*, 1990), and the Dead Sea (Al-Zoubi & Ten Brink, 2001).

Examples of ancient preserved sedimentary successions considered to have been influenced by subsurface salt halokinesis are the shallow-marine Wonoka Formation of the Flinders Range, Australia (Kernen *et al.*, 2012), La Popa Basin, Mexico (Aschoff & Giles, 2005), the deep-marine Bryant Canyon, Garden Banks, Gulf of Mexico (Fiduk, 1995), and Eugene Island and Ship Shoal, Gulf of Mexico (Hall & Thies, 1995). Fluvial successions interpreted to have been influenced and controlled by ongoing halokinesis include those of the Triassic of the Central North Sea (Smith *et al.*, 1993; Jones *et al.*, 2005; McKie & Audretsch, 2005), the Triassic Pre-Caspian Basin, Kazakhstan (Barde *et al.*, 2002; Hinds *et al.*, 2004), the Eocene Carroza Formation, La Popa Basin, Mexico (Andrie *et al.*, 2012), and the Pennsylvanian-Jurassic Salt Anticline Region of the Paradox Basin, SE Utah (Hudec, 1995; Lawton & Buck, 2006; Prochnow *et al.*, 2006; Matthews, 2007; Trudgill, 2011). The fluvial succession of the Lower Triassic Moenkopi Formation present in the mini-basins of the Salt Anticline Region of the Paradox Basin is the focus of this study.

The aim of this study is to document the mechanisms by which styles of basin subsidence and related salt-wall growth act to directly control fluvial-system type and the form of the stratigraphic architecture preserved in a series of mini-basins. This has been achieved through a detailed analysis of the outcrop pattern of the Triassic Moenkopi Formation, a hybrid braided-channel and non-confined sheet-like fluvial system that developed under the influence of an arid climate across much of what is now the south-western United States region (Ward, 1901; Darton, 1910; Gregory, 1917; Stewart, 1959; Stewart *et al.*, 1972; Blakey, 1974). The study accomplishes the following objectives: (i) demonstrates changes in fluvial style between adjacent mini-basins and shows how surface topography generated by salt-wall uplift was able to effectively partition the fluvial system into sand-prone fairways dominated by stacked complexes of channel architectural elements, and extensive areas that were relatively sand-starved and dominated by complexes of fine-grained sheet-like architectural elements; (ii) demonstrates how the distribution of associations of fluvial lithofacies and architectural elements varies predictably from the centre of subsiding mini-basins onto the

flanks of bounding salt walls; (iii) illustrates how analysis of the occurrence of associations of fluvial lithofacies and the distribution of architectural elements can be used to infer the relative timing of episodes of salt-wall uplift versus episodes of quiescence through the recognition of styles of onlap and erosional truncation of packages of fluvial elements; (iv) demonstrates how the preserved fluvial succession evolved temporally as accommodation within the evolving mini-basins became progressively infilled.

### ***Background and Geological Setting***

The Paradox Basin developed from the Pennsylvanian to Permian as an intra-foreland flexural basin in response to lithospheric loading by the Uncompahgre Uplift, which formed as part of the so-called Ancestral Rocky Mountains (Fig. 1), one of several late Palaeozoic features developed during the Ancestral Rocky Mountain orogenic event (Ohlen & McIntyre, 1965; Kluth & Coney, 1981; Barbeau, 2003). The Uncompahgre Uplift was ~145 km long and elongated in a northwest-southeast orientation across southwest Colorado and southeast Utah (Elston *et al.*, 1962). From the mid-Pennsylvanian to the late-Permian, in excess of 4000 m of strata accumulated in the foredeep, directly adjacent to the frontal thrust that bounded uplifted Precambrian basement rocks of the Uncompahgre Uplift (Elston *et al.*, 1962). Erosion of the Uncompahgre Uplift yielded much of the clastic detritus that filled the proximal part of the Paradox Basin, resulting in the south-westward progradation of a large alluvial clastic wedge (Mack & Rasmussen, 1984; Barbaeu, 2003). During the initial stages of formation, the foredeep of the Paradox Basin experienced a series of transgressive-regressive events and cycles accumulated in response to glacio-eustatic sea-level changes recorded by the pattern of sedimentation in the Hermosa Group (Goldhammer *et al.*, 1991; Blakey & Ranney, 2008; Williams, 2009). During episodes of falling relative sea-level, the basin was partially isolated from a regional sea-way by the basin fore-bulge, causing dense brines to develop in the foredeep of the basin. Repeated desiccation and recharging of these brines resulted in accumulation of the Paradox Formation (Doelling, 1988), a unit characterised by cyclic deposits of salts (anhydrite, halite and potash) interbedded with marls and black shales (Hite, 1968; Williams-Stroud, 1994; Rasmussen &

Rasmussen, 2009). From the late Pennsylvanian (Missourian to Virgilian) to the early Permian (Wolfcampian), the growing alluvial clastic wedge constructed from detritus derived from the eroding Uncompahgre Uplift prograded further into the foreland basin, though alluvial sedimentation was periodically repeatedly interrupted by widespread marine incursions that gave rise to the accumulation of thin but laterally extensive shallow-marine carbonate intervals throughout the Missourian to Wolfcampian, as represented by the Honaker Trail Formation (Williams, 1996, 2009) and the overlying lower Cutler beds (Blakey 2009; Jordan & Mountney, 2010, 2012).

Initial movement of the salt layers of the Paradox Formation occurred in response to loading by sediments of the Honaker Trail Formation and lower Cutler beds during late-Pennsylvanian and early Permian (Trudgill *et al.*, 2004), as demonstrated by structural basin modelling (Paz *et al.*, 2009; Rasmussen & Rasmussen, 2009; Kluth & Du Chene, 2009; Trudgill, 2011). The sites of initiation of salt-wall development were controlled by a series of normal faults aligned in an orientation parallel to the Uncompahgre Front: these faults were activated by flexural downwarping of the developing foredeep (Baars, 1966, Friedman *et al.*, 1994; Doelling, 2002b). Similar basement-fault arrays control the geometries of growing salt-walls in the Central North Sea (Smith *et al.*, 1993; Hodgson *et al.*, 1992). As the effects of sediment loading continued to drive subsurface salt withdrawal and migration into a series of growing salt walls, so a series of salt-walled mini-basins began to develop (Fig. 1), initially in the foredeep of the Paradox Basin where the salt layers of the Paradox Formation were thickest and the thickness of overburden greatest (Jones, 1959). Accelerated rates of mini-basin development and ensuing salt-wall growth occurred in the proximal-most part of the Paradox Basin in response to additional sediment loading associated with the progradation of a thick alluvial clastic wedge of the Cutler Group, an alluvial mega-fan that prograded south-westward into the basin from the Uncompahgre Uplift (Mack & Rasmussen, 1984; Barbeau, 2003; Cain & Mountney, 2009, 2011; Trudgill, 2011). The proximal part of the alluvial clastic wedge of the so-called undifferentiated Cutler Group (Newberry, 1861; Dane, 1935), which accumulated during the main phase of mini-basin evolution,

exhibits substantial thickness variation between mini-basins and over salt walls (Trudgill, 2011). Fluvial deposits of this unit demonstrate abrupt and repeated changes in palaeoflow direction that can be shown to have been directly influenced by concomitant salt-wall growth and basin subsidence (Trudgill, 2011; Venus *et al.*, in review). Salt withdrawal from beneath the basins occurred at the greatest rates adjacent to the developing salt walls, eventually culminating in grounding of the floor of the basins on underlying basement beneath these points and resulting in the trapping of salt remaining beneath the centres of the mini-basins. This resulted in the formation of rim synclines at the basin peripheries (Smith *et al.*, 1992; Doelling, 2002b; Trudgill & Paz, 2009; Trudgill 2011). Salt movement via withdrawal from beneath subsiding mini-basins and its lateral migration to maintain growing salt-walls continued throughout the Triassic and Jurassic, although at a significantly reduced rate compared to that during the Permian (Trudgill, 2011).

Throughout the early Triassic (Induan to Olenekian - Morales, 1987; Rasmussen & Rasmussen, 2009), the Moenkopi Formation accumulated across a laterally extensive area now represented by large parts of the states of Arizona, New Mexico, Colorado, Utah and Nevada (Ward, 1901; Darton, 1910; Gregory, 1917; Stewart, 1959; Cater, 1970; Blakey, 1974, 1989; Hintze & Axen, 1995). Regionally, this formation accumulated in an overall mixed fluvial and paralic (coastal) setting, with a region-wide marine regression dictating the style of sedimentation (Blakey, 1973). In the Salt Anticline Region (Fig. 2), the Moenkopi Formation has been the subject of several previous studies, most notably by Baker *et al.* (1927), Dane (1935), and Shoemaker & Newman (1959). Here, the Moenkopi Formation consists of four members: the Tenderfoot, Ali Baba, Sewemup and Parriott (Fig. 3; Shoemaker & Newman. 1957 & 1959). The name "Parriott" has been used here to reflect the current cartographic convention; this differs from "Pariott" as used by Shoemaker & Newman (1959).

The provenance of sediment of the Moenkopi Formation in the Salt Anticline Region varies between the mini-basins indicating that uplifted salt walls were effective in partitioning fluvial systems with different source areas. The

Uncompahgre and the San Luis uplifts to the northeast and southeast, respectively (Fig. 1), were the principal sediment sources and these uplifts represented the only significant upland areas from which palaeo-fluvial systems likely originated (Cadigan & Stewart, 1971; Mattox, 1968; Stewart *et al.*, 1972; Barbeau, 2003). Although at a regional scale the Moenkopi Formation records accumulation in a mixed fluvial and paralic setting, with conditions becoming increasingly marine-influenced towards the northwest (Blakey, 1973), the environment of deposition in the Salt Anticline Region is considered to be that of an arid alluvial plain over which ephemeral streams passed toward a regressing palaeo-shoreline that lay 100 to 300 km the northwest, in the area now occupied by Central Utah (Stewart *et al.*, 1972; Lawton & Buck, 2006; Blakey & Ranney, 2008). The Moenkopi Formation in the study region represents the preserved succession of a largely non-confined alluvial braidplain that preserves a mix of sheet-like and braided-channel fluvial sedimentary architectures.

### ***Methods and Data Collection***

Fifty-two sections were measured in the Salt Anticline Region, recording a total of ~9000 m of succession from the Moenkopi Formation (see Fig. 2 for log locations and Fig. 4 for representative examples). Of these, 23 measured sections record the entire preserved thickness of the Moenkopi Formation from the top of the underlying Undifferentiated Cutler Group to base of the overlying Chinle Formation; all other sections record significant proportions of the succession, including either the base or top of the formation in each case.

Sixteen distinct lithofacies are recognised (Table 1; Fig. 5), of which most are interpreted to have been generated by a range of fluvial behaviour involving both channelised and non-channelised flow processes; some lithofacies are ascribed to non-fluvial origins in related palaeoenvironmental settings, including shallow, ephemeral lakes and salt flats. Architectural elements (Fig. 6) have been defined according to their geometry and their internal lithofacies composition based on the approach described by Miall (1985, 1996). Palaeocurrent data were collected to determine the direction of drainage: 177 indicators of flow direction were taken from asymmetric ripple casts (Frc),

climbing ripple strata (Frc/Fxl), trough cross-bedding (Fxt) and high-angle-inclined planar cross-bedding (HA Fxp). From these palaeocurrent data, vector mean and vector magnitude were calculated using the methodology described by Lindholm (1987).

Scaled drawings (panels) depicting the distribution of fluvial architectural elements both within a single mini-basin and between adjacent mini-basins have been constructed by lateral tracing and correlation of key surfaces in the field and supported by analysis of photomontages. Architectural panels have been tied to measured sections to enable the generation of a series of models with which to depict important tectono-stratigraphic relationships.

### ***Styles of mini-basin fill***

The sedimentary record of the style of interaction between mini-basin subsidence and salt-wall growth due to subsurface halokinesis is recorded in the preserved pattern of deposition of coevally active fluvial systems in three studied mini-basins, the Fisher Basin, the Parriott Basin and the Big Bend Basin (Figs 2 & 3). Tectono-stratigraphic interactions are especially evident in areas adjacent to salt walls (Fig. 7a, b), where fluvial architectural elements of various types ramp onto, or terminate against salt-wall uplifts. Correlations of the four members of the Moenkopi Formation, both within individual mini-basins and between adjacent mini-basins (Fig. 8a, b, c), demonstrate the basin-scale architecture of the fluvial fill, relationships within which document the history of accumulation (Fig. 9).

### **The Fisher Basin**

#### *Description*

The Fisher Basin, which is situated adjacent to the Uncompahgre Front, is filled predominantly with 4,000 m of sediment of the Pennsylvanian to Permian Honaker Trail Formation and Cutler Group (Trudgill, 2011). The thickest development of the Moenkopi Formation in the Fisher Basin is ~125 m, which is the thinnest preserved succession of Moenkopi Formation in the studied mini-basins of the Salt Anticline Region. An angular unconformity at the base and a disconformity at the top of the Moenkopi Formation are well exposed in the Richardson Amphitheater area and at Fisher Towers. The

thickest preserved accumulation of Moenkopi Formation in the Fisher Basin is in a rim syncline developed on the north side of the Fisher Valley salt wall, development and infilling of which occurred predominantly during the Permian (Doelling, 2002a; Trudgill & Paz, 2009).

The basal-most Tenderfoot Member in the Fisher Basin is 30 to 40 m thick and is characterised by massive beds of medium-grained sandstone that are present across the entire basin, with little variation in thickness over 10 km. Associated crinkly laminated units of medium-grained sandstone of uncertain origin are additionally present at some locations within the mini-basin. Channel elements are difficult to discern as the member is largely homogeneous with respect to grain-size. A prominent but regionally restricted, 1.5 m-thick gypsum bed is present 5 m above the base of the Moenkopi Formation in the Cottonwood Canyon area, but elsewhere in the basin has been largely removed by erosion.

The overlying Ali Baba Member is 50 to 70 m thick and is characterised by multi-lateral and multi-storey, amalgamated channel-fill elements of medium- to coarse-grained sandstone and conglomerate that represent the coarsest-grained units of significant thickness in the Moenkopi Formation of the Salt Anticline Region. Amalgamated channel elements (F1; Fig. 6) are composed of planar and trough cross-bedded strata (Fxp & Fxt). The basal-most part of the member is composed of crudely cross-bedded paraconglomerates (Fxt & Fce) with clasts of extraformational origin. The middle part is composed of medium- to coarse-grained, cross-bedded sandstone (Fxt/HA Fxp), beds of which contain intra- and extraformational clasts (Fci/e) as either basal lags or as floating clasts. The upper part is characterised by increasing occurrences of sheet-like elements (F3) composed of climbing-ripple strata (Frc) and heterolithic strata (Fhiss), especially in the uppermost 5 to 20 m of the succession, where channel elements are scarce.

Although the Sewemup Member is present in the Fisher Basin, it lacks gypsum-clast-bearing beds (FGc/m) that are a diagnostic feature in other mini-basins; it is instead characterised by heterolithic siltstones and

sandstones expressed as sheet-like elements (F3), with only rare and vertically isolated single-storey channel elements (F2; Fig. 6).

The Parriott Member is absent across the Fisher Basin; the disconformity at the top of the Moenkopi Formation incises up to 25 m into the top-most part of the Sewemup Member (Fig. 8b). Palaeocurrent readings ( $n = 88$ ) taken from all members in the Fisher Basin record a vector mean of  $305^\circ$  (vector magnitude = 90.8%), indicating that palaeoflow was aligned parallel to the axis of the salt wall throughout duration of Moenkopi deposition.

### *Interpretation*

The majority of the Fisher basin is filled by the deposits of the Honaker Trail Formation and the Undifferentiated Cutler Group, the coarse-clastic detritus, was likely exclusively sourced from the adjacent Uncompahgre Front, with no salt-walls having been present to divert or impede the delivery of pebble- and cobble-grade detritus into the mini-basin via proximal fluvial systems (Trudgill, 2011; Venus et al., in review). The relatively thin accumulation of the Moenkopi Formation in the Fisher Basin compared to that of the Parriott and Big Bend basins (described later) arose in part because subsidence of Fisher Basin ceased relatively early in the history of the halokinetic evolution of the area: the rim syncline of the Fisher Basin adjacent to the Fisher Valley salt wall had grounded or was close to grounding on the pre-salt strata by the onset of accumulation of the Moenkopi Formation (Trudgill & Paz, 2009). This resulted in a slow rate of subsidence for the Fisher Basin during the early Triassic, whereby only ~120 m of accommodation was generated and infilled. The source of the fluvially derived sediment filling the basin during accumulation of the Moenkopi Formation was likely a combination of sediment derived from the Uncompahgre Front to the northeast and from the San Luis uplift in the south (Cater, 1970; Stewart *et al.*, 1972). The prominent gypsum bed likely accumulated as a precipitate from an evaporating brine pool that developed in the embayment formed by the developing mini-basin, or developed as a sabkha type deposit, with salt from the underlying wall acting as the source of the salt. In the majority of the basin, significant parts of this bed were eroded by fluvial incision and dissolution prior to renewed

sedimentation. Throughout the episode of time represented by the accumulation of the Moenkopi Formation, the Fisher Basin apparently evolved from a sand-prone to a progressively sand-poor basin, as demonstrated by an upward decrease in the sand content of the succession. This change in basin-fill style was likely principally driven by a progressive reduction in the rate of sediment supply from the gradually denuding Uncompahgre Uplift. By the time of accumulation of the Parriott Member, the Uncompahgre Uplift was largely denuded (Blakey & Ranney, 2008; Blakey, 2009) and was no longer a significant source of sediment to the Fisher Basin. The originally accumulated thickness of the Parriott Member in the Fisher Basin remains unknown, though the unconformity at the base of the overlying Chinle Formation has regional relief of no more than 25 m (Fig. 8a), which constrains the maximum likely thickness of the Parriott Member in the Fisher Basin. However, the inferred reduced rate of sediment delivery to the basin could have precluded deposition of the Parriott Member completely.

## **The Parriott Basin**

### *Description*

The thickness of Moenkopi Formation in the Parriott Basin varies from 140 m adjacent to the Onion Creek – Fisher Valley salt wall, to 180 m in the centre of the mini-basin at the Priest and Nuns mesas, to 220 m in a rim syncline developed adjacent to the Castle Valley salt wall (Fig. 8c). The succession thins to less than 30 m directly adjacent to the nose of the Castle Valley salt wall itself (Fig. 8b). Two rim synclines formed in the Parriott Basin: one in the northeast, adjacent to the southwest flank of the Fisher Valley salt wall, and another to the southwest, adjacent to the northeast of the Castle Valley salt wall (Doelling, 2002a; Trudgill 2011). In the north-eastern rim-syncline (adjacent to Fisher Valley salt wall), the Moenkopi Formation exhibits neither thickening of the succession nor any variations in lithofacies or architectural-element distribution. In the south-western rim-syncline (adjacent to Castle Valley salt wall), the Moenkopi Formation thickens by 30 m into the local depocentre and is characterised by an increased abundance of fluvial channel elements in the Ali Baba and Parriott members compared to the equivalent intervals in the centre of the mini-basin.

The accumulated succession in the Parriott Basin is dominated by sheet-like architectural elements (F3), composed of laterally extensive, horizontally interbedded siltstones and sandstones (Fhiss), with minor occurrences of massively bedded sandstones (Fm). The basal-most Tenderfoot Member is characterised by a distinctive 1.5 to 2.5 m-thick gypsum bed, which is also present in the part of the Fisher Basin and in the Big Bend Basin. This gypsum horizon is laterally continuous throughout the Parriott Basin, being well exposed on both the Castle Valley and Fisher Valley sides of the basin. The gypsum horizon is characterised by a saccharoidal, crystalline texture and in several places contains deformed internal stratification, though elsewhere is massive (no internal structure), or is characterised by sigmoidal cross-bedding (Lawton & Buck, 2006).

Interbedded facies associations are particularly notable in the Sewemup Member where they are associated with ubiquitous pebble- and cobble-grade gypsum-clast-bearing beds (FGc/m). These gypsum-clast-bearing units are unique to the Sewemup Member and are most prevalent in areas within 4 km of the margins of the Castle Valley salt wall but are absent from areas adjacent to the Fisher Valley salt wall.

The Parriott Member is characterised by single-storey, multi-lateral channel elements (F2) that are preferentially clustered immediately adjacent to the Castle Valley salt wall in the rim-syncline. The member is of uniform thickness across much of the basin but it doubles in thickness from 30 m to 60 m in the area adjacent to the Castle Valley salt wall where the pronounced rim syncline is developed (Trudgill, 2011). Palaeocurrent indicators throughout the Moenkopi Formation in the Parriott Basin indicate fluvial transport toward a mean vector of  $303^\circ$  (vector magnitude = 85%;  $n = 57$ ), indicating a dominant palaeoflow that was parallel to the trend of the axis of the mini-basins.

### *Interpretation*

The variation in thickness of the Moenkopi Formation in the Parriott Basin demonstrates that the basin underwent an asymmetric pattern of subsidence

during accumulation of both the underlying Cutler Group and the overlying Moenkopi Formation. During accumulation of the Cutler Group, transport and deposition occurred in a south-westerly direction (Cain and Mountney, 2009; Venus *et al.*, in review), with overall sediment transport generally being in a direction perpendicular to the trend of the developing salt walls. This indicates that the rate of fluvial sedimentation generally outpaced the rate of salt-wall uplift such that fluvial systems of the Undifferentiated Cutler Group were not influenced by salt-induced surface topography throughout much of their evolution (Venus *et al.*, in review).

Increased subsidence rates in the rim synclines of the Parriott Basin were driven by loading from a thicker overburden deposited by the prograding fan of the Undifferentiated Cutler Group. Accelerated salt withdrawal resulted in the development of rim synclines on both the Fisher Valley and Castle Valley sides of the Parriott Basin. These rim synclines continued to develop throughout accumulation of the Cutler Group before subsidence in the north-eastern rim syncline (adjacent to the Fisher Valley salt wall) ceased, apparently before salt-weld formation occurred (Trudgill & Paz, 2009; Trudgill, 2011). By contrast, the south-western rim syncline (adjacent to the Castle Valley salt wall) continued to subside throughout the period represented by accumulation of the Moenkopi Formation, resulting in the development of an asymmetric style of basin-fill (Fig. 8c).

During Accumulation of the Moenkopi Formation, subsidence rates were greater in the Parriott Basin than in the Fisher Basin, which enabled the former to accommodate a significantly thicker accumulation of Moenkopi succession: a maximum of 220 m versus a maximum of only 125 m in the Fisher Basin. The gypsum bed in the Tenderfoot Member likely accumulated in either a restricted tidal-flat (sabkha) setting or within an embayment with restricted opening that was subject to repeated flooding and desiccation (Stewart *et al.*, 1972). In places, sediment from this gypsum bed has been interpreted to have been partially reworked to form a cross-bedded aeolianite (Lawton & Buck, 2006). Palaeocurrent data demonstrate fluvial flow occurred parallel to the axis of the mini-basin (to the northwest), indicating that the

Parriott Basin was isolated from much of the detritus being shed from the Uncompahgre Front during Moenkopi deposition, either because fluvial systems emanating from the remnant Uncompahgre highlands did not extend this far into the Paradox Basin or, more likely, because uplift of the Fisher Valley and Sinbad Valley salt walls generated a surface topography that was sufficient to prevent such fluvial systems reaching the Parriott Basin (Fig. 1). This limited the primary source of sediment for the Parriott Basin to that of the San Luis range to the southwest (Cadigan & Stewart, 1971). The likely isolation of the Parriott Basin from the Fisher Basin by an elevated salt-wall topography, meant that the rate of sediment delivery to the former was limited and the rate of filling of accommodation was therefore likely low relative to rate of basin subsidence during early- to mid-stages of accumulation of the Moenkopi Formation, resulting in a basin fill characterised by argillaceous, sheet-like elements (F3) interbedded with only minor sandstone elements (F2) in the Ali Baba, Sewemup and Parriott Members (Fig. 6).

High rates of basin subsidence, and associated ensuing high rates of salt-wall uplift at the basin margins relative to the low rate of filling of accommodation in the central parts of the basin culminated in the uplift of the Castle Valley salt wall to a level where it breached the land surface during accumulation of the Sewemup Member, whereupon it acted as a local source of gypsum detritus, which was re-worked into the strata surrounding the Castle Valley salt wall as discrete gypsum-clast-bearing beds (Lawton & Buck, 2006). The absence of gypsum clasts from the Moenkopi succession at the margins of the Fisher Valley salt wall demonstrates that this halokinetic feature did not breach the land surface during deposition of the Moenkopi Formation (Fig. 8c). The confinement of gypsum pebbles and cobbles to within 7 km of the Castle Valley salt wall (with orthoconglomerate beds occurring closer to the salt wall) indicates that alluvial processes were not able to distribute the detrital gypsum clasts evenly over the entire basin floor (Fig. 8c). During accumulation of the Parriott Member, preferential subsidence during the final phase of salt withdrawal adjacent to Castle Valley salt wall (Trudgill, 2011) resulted in the renewed development of a rim syncline and the preferential preservation of single-storey channel elements (F2) in this local depocentre (Fig. 8c).

## The Big Bend Basin

### *Description*

Deposits in the Big Bend Basin are not as well exposed as those in the other studied mini-basins, with the full thickness of the Moenkopi Formation succession (235 m) only exposed along the south-western flank of the Castle Valley salt wall, and the succession thinning to less than 30 m thick adjacent to the nose of the Castle Valley salt wall (Fig. 7a, b). The base and top of the Moenkopi Formation are not seen at other single geographic localities in the Big Bend mini-basin and the true maximum thickness of the Moenkopi Formation in this basin is therefore uncertain.

On the south-western flank of the Castle Valley salt wall, a prominent angular intraformational unconformity with a discordance of  $\sim 6^\circ$  is present between the Tenderfoot and Ali Baba members (Fig. 7b). The basal gypsum unit is not present in the Tenderfoot Member immediately adjacent to the salt wall, though it is present elsewhere in the Big Bend Basin. Toward the centre of the basin, near the Big Bend campground, only the upper part of the Sewemup Member and the full succession of the Parriott Member are exposed. Gypsum-clast-bearing beds are present in the Sewemup Member at the Big Bend campground locality, a distance of 2.8 km from the Castle Valley salt wall. The Parriott Member at Big Bend Campsite C has a thickness of 70 m, which is the thickest observed preserved succession of Parriott Member in the study area.

Adjacent to the Castle Valley salt wall, at the north east edge of Matt Martin Point (Fig. 2), a series of well-developed channel elements are preserved as overlapping multi-lateral and twin- or multi-storey channel complexes (F1). Toward the centre of the mini-basin, near the Red Cliff Lodge road section, the Parriott Member comprises amalgamated channel elements (F1 & F2) composed internally of trough- (Fxt) and planar-cross bedded (Fxp) sets with intraformational clasts (Fci). These elements overlie a succession of interbedded siltstones and sandstones (Fhiss) with a sheet-like geometry (F3), and are themselves overlain by thin interbedded sandstone and siltstone

heterolithic sheet-like elements (F3), the upper parts of which are cut-out by the disconformity at the base of the Chinle Formation.

### *Interpretation*

The presence of the intraformational unconformity between the Tenderfoot and Ali Baba members demonstrates a temporary cessation in sedimentation, during which time salt-wall uplift was ongoing. During accumulation of the Ali Baba Member, the fluvial system aggraded and encroached onto the flanks of the salt wall, locally reworking the uplifted succession of the Tenderfoot Member and generating the angular unconformity. A rim syncline had developed in the Big Bend mini-basin immediately adjacent to the flank of the Castle Valley salt wall by the time of accumulation of the Parriott Member (Fig. 8); this resulted in the preferential stacking and clustering of vertically and laterally amalgamated channel elements (F1) adjacent to the Castle Valley salt wall, but their absence in central parts of the basin (e.g. Big Bend Campsite C). The gypsum-clast-bearing horizons observed in the Sewemup Member toward the basin centre indicate that gypsum detritus was shed into the Big Bend Basin (in addition to the Parriott Basin) from the actively uplifting Castle Valley salt wall. The presence of gypsum clasts throughout the central part of the Big Bend mini-basin demonstrates that this detritus was reworked and re-distributed by fluvial systems in the mini-basin. The thickness of the preserved Sewemup Member succession is similar in both the Parriott and Big Bend mini-basins, demonstrating that the basins on either side of the Castle Valley salt wall underwent similar rates of subsidence. The different styles of preserved sedimentary architecture of the Parriott Member in the Big Bend and Parriott basins indicates that the fluvial systems were isolated from each other by the Castle Valley salt wall.

## **Styles of salt-wall and sediment interaction**

### **The Fisher Valley salt wall and Onion Creek salt diapir**

Due to recent erosion, little direct evidence remains with which to demonstrate the style of interaction between the pattern of sedimentation in the Moenkopi Formation and the synchronous evolution of the Fisher Valley salt wall. To the north of this salt wall, near-horizontally bedded outcrops are largely

inaccessible where they form sheer cliffs at Fisher Towers (1.5 km from the edge of the Fisher Valley salt wall). To the south of the Fisher Valley salt wall, the closest outcrop of the Moenkopi Formation is 600 m from the margin of the salt wall and here beds are again near-horizontal. Thus, deformation of the accumulated strata by the uplifting salt wall was restricted solely to the immediate margins of the wall.

## **The Castle Valley salt wall**

### Description

Well exposed outcrops that demonstrate direct evidence for the interaction between sedimentation in the Moenkopi Formation and synchronous salt-wall growth are present in the Red Hills area (known locally as the “Truck and Boat”) at the northern margin of the Castle Valley salt wall (Fig. 7a). The style of salt-wall uplift is asymmetric in nature, with the Pre-Triassic sediments of the Cutler Group having been uplifted to a greater height on the western side of the salt wall than on the eastern side. The asymmetric nature of the uplift is further demonstrated by the geometries of the uplifted salt-wall flanks: the eastern flank of the uplift, which forms the bounding edge of the Parriott Basin, exhibits a horizontal-inclined-horizontal geometry, whereas the western flank, which forms the bounding edge of the Big Bend Basin, exhibits a simpler, wedge-like geometry (Fig. 7b).

The horizontal-inclined-horizontal geometry that characterises the eastern flank of the Castle Valley salt wall (Fig. 7a; east side) is related to a narrow zone of deformation. Two inflection points, a convex bend adjacent to the crest of the salt wall and a concave bend at the down-dip margin of the feature at a point where the succession moves off the salt-wall flank, define a monocline (Lawton & Buck, 2006). The sedimentary succession on top of the salt wall is near-horizontal, whereas inclined strata on the flank of the salt wall dip away from the crest at an angle up to 23° toward 114°. Figures 7a demonstrate the extent of the thinning onto the Castle Valley salt wall: the thickness of the succession between the middle of the Ali Baba Member and beds in the upper part of the Parriott Member thins by 30 m over a distance of 445 m from the crest of the salt wall, eastwards to a point at the limit of salt-

wall-related deformation, giving an approximate rate of thinning of 1 in 14. The aforementioned beds in the upper part of the Parriott Member have been uplifted by 76 m on to the crest of the salt wall relative to their lateral equivalent beyond the zone of salt-wall deformation. Within the accumulated strata on the eastern flank of the Castle Valley salt wall, sand-prone fluvial channel elements ramp up onto the salt wall, thinning or pinching-out as they onlap onto the upper flanks of the structure (Figs 7b & 9b). On the eastern flank of the Castle Valley salt wall, beds of the Ali Baba Member with a distinctive grey colouration due to reduction of beds with wave-rippled surfaces are present (Fig. 9b). In the upper part of the Sewemup Member and the lower part of the Parriott Member, shearing of some of the sand-prone channel elements is present adjacent to the salt wall (Fig. 9b).

The slope geometry that characterises the western flank of the Castle Valley salt wall dips gently towards the west into the Big Bend Basin and is characterised by fanning growth strata that thin onto the crest of the salt wall (Fig. 7b). At the unconformity between the underlying sediments of the Cutler Group and the base of the Moenkopi Formation, a series of 3 growth-faults, each of which exhibit displacement of up to 2.5 m, are developed in the strata that form the uppermost part of the Cutler Group (preserved locally as a distinctive white-coloured aeolianite that might be equivalent to the White Rim Sandstone present in more distal parts of the Paradox Basin – Venus et al., in review). These faults, which strike at 197°, parallel to the uplift at the end of the salt wall, have displacements of 1 to 2 m, have hanging-walls that dip away from the salt-wall and are filled with poorly bedded medium-sandstone (Fm) of the Tenderfoot Member.

Two sedimentary sections recording laterally equivalent parts of the Tenderfoot and basal-most Ali Baba Member on the west flank (Fig. 7b) demonstrate thinning of 30 m over a lateral distance of 270 m, from 72 m at the West Flank Gully log located part-way down the flank of the salt wall, to 42 m at the West Flank Spur log close to the crest of the salt wall (Fig. 7b), yielding an average rate of thinning of 1 in 9. The top of the succession adjacent to the salt wall has been elevated by 21 m relative to the equivalent

part of the succession in the log 270 m away. The density of occurrence of single-storey channel elements (F2) filled with massive sandstone (Fm) systematically decreases with increasing proximity to the salt wall (Fig. 7b). Several major channel elements that are laterally continuous in the Big Bend rim syncline thin and pinch-out as they onlap onto the upper flank of the Castle Valley salt wall. Around the rest of the valley, other inferred onlap relationships are not well preserved due to erosion.

### Interpretation

The Castle Valley salt wall formed an elevated topographic feature that acted to effectively partition and isolate the Parriott and Big Bend mini-basins throughout the majority of the episode of sedimentation represented by the Moenkopi Formation; the margin of the Big Bend Basin is sand-prone whereas the margin of the Parriott Basin is relatively sand-poor. The overall thinning of the strata onto the flanks of the Castle Valley salt wall demonstrates that uplift occurred synchronously with sedimentation. Present-day differences in height between known stratigraphic levels recorded in the logged sections demonstrate continued post-depositional salt-wall uplift. The thinning and pinch-out of channel elements onto the upper flanks of the salt wall indicate that fluvial systems were actively diverted by the uplifted salt wall for significant episodes during accumulation of the Moenkopi Formation. The effective partitioning of the Parriott and Big Bend basins during accumulation of the Parriott Member is demonstrated by differences in basin-fill style either side of the salt wall: the Parriott Member is significantly more sand prone in the Big Bend mini-basin, where multi-storey channel elements (F1) are preserved adjacent to the salt wall but at an equivalent stratigraphic level in the Parriott Basin, only thin and isolated single-storey channel elements (F2) occur intercalated with heterolithic sheet-like elements (F3). Preserved wave-ripple forms on bedding surfaces in the Ali Baba Member on the east flank of the Castle Valley salt wall are indicative of standing water on this now uplifted section of salt wall. This likely indicates that, at some point during Ali Baba deposition, the Castle Valley salt wall was present only in the sub-surface and the topographic expression of the salt wall was sufficiently subdued to allow water to pond in the area directly above the salt wall. In the upper part of the

Sewemup Member and the lower part of the Parriott Member, shearing of some sand-prone channel elements in a style indicative of growth-fault development indicates that the salt wall was still growing after accumulation of these members (Fig. 9b). The orientation of the growth faults present on the western flank of the Castle Valley salt-wall, together with their style of displacement, required early cementation and brittle deformation of strata of the White Rim Sandstone in which these features are developed. Displacement was likely associated with phases of salt-wall uplift or mini-basin subsidence, as demonstrated by down-throw on the basinward side, with the generated space subsequently being filled by sediment younger sediment of the Monekopi Formation. This indicates either that salt-wall uplift was responsible for elevating the growth-fault footwalls, or that salt evacuation in the developing rim syncline was responsible for lowering the hanging walls, or a combination of both.

### **Cache Valley salt-wall**

The Cache Valley salt wall (Fig. 2) is thought to have been linked to the Fisher Valley salt wall by a section of salt swell with subdued relief present only in the subsurface (Shoemaker, 1955). This subdued segment of the salt wall running between the end of Onion Creek and Cache Valley is overlain by a small uplifted outcropping section of the Moenkopi Formation. The structural feature that links these salt walls might be the expression of a relay ramp that joined two pre-salt fault systems, and which was responsible for accumulating a differential thicknesses of salt on either side of the structure; such a feature might have served as a trigger for the initiation of salt-wall growth (cf. Hodgson *et al.*, 1992; Doelling, 2002a).

### ***Tectono-stratigraphic model***

Based on observations regarding the sedimentology and stratigraphy of the preserved succession and its relationship to the various subsiding mini-basins and uplifting salt walls, the tectono-stratigraphic evolution of the Moenkopi Formation in the studied part of the Salt Anticline Region has been reconstructed. Detailed relationships established from analysis of field-derived data have enabled a suite of models describing the evolution of the province

as a whole to be reconstructed (Fig. 10a); tectono-stratigraphic relationships within individual mini-basins have been established (Fig. 10b), and the character of individual fluvial architectural elements has been discerned (Fig. 10c, d). Furthermore, a series of spatio-temporal evolution models has been developed for the three studied mini-basins and their bounding salt walls; the proposed models account for the distinctive styles of basin fill (Figs 11, 12, 13), such that differences in preserved fluvial architectural style can be attributed to the dynamic interplay between rates of sediment delivery and accumulation, rates of mini-basin subsidence, and rates and styles of associated salt-wall uplift.

### **Tenderfoot Member**

During accumulation of the Tenderfoot Member, sedimentation in the three studied mini-basins was dominated by the accumulation of structureless sandstones, accumulation of which was influenced by evaporite precipitation as indicated by the presence of the distinctive 1.5 to 2.5 m-thick gypsum bed in all three basins, albeit in only a partially preserved state in the Fisher Basin (Figs 11a, 12a, 13a). The origin of the gypsum could be via (i) precipitation from a super-saturated brines in evaporating salt pans in the restricted basins (Sloss, 1969), or (ii) dissolution of gypsum from within the salt wall, with gypsum-brine then being drawn to the ground surface by capillary action, whereupon evaporation and precipitation led to the accumulation of a sabkha-like pan deposit (Selley, 1988). The deposit was apparently locally reworked by the wind to form a gypsum aeolianite in the Parriott Basin (Lawton & Buck, 2006). In the Fisher Basin, where the gypsum bed was either only sporadically deposited, or was subsequently removed by erosion associated with fluvial activity, crinkly laminated sandstones (Scls) are present, indicating disturbance of the sediment by ground water being drawn upward by capillary action and evaporation at the ground surface (cf. Goodall *et al.*, 2000). Similar sandstone deposits are present in the Parriott Basin directly above the gypsum horizon, where precipitated gypsum forms a weak sandstone cement.

In the Big Bend Basin, growth strata are present at the base of the Tenderfoot Member in small faults at the very top of the aeolianite at the top of the Cutler

Group (Fig. 13b). This indicates that the aeolianite (possibly equivalent to the White Rim Sandstone) in this locality had lithified to a point where brittle deformation could take place, and sediment of the Tenderfoot Member accumulated as growth strata within the growing fault-bounded hanging-walls. The prominent intraformational unconformity present locally at the top of the Tenderfoot Member in the Big Bend Basin indicates a hiatus in sedimentation between deposition of the Tenderfoot and Ali Baba Members, during which time salt-wall uplift continued (Fig. 7b).

### **Ali Baba Member**

The sedimentary style of the Ali Baba Member is indicative of an episode of significantly increased fluvial activity in all three mini-basins, which is recorded as a series of multi-storey, multi-lateral channel elements (F1) in the Fisher Basin, and single storey channel elements, with sand-prone sheet-like heterolithic units in the Parriott Basin. Paraconglomerates in the Fisher Basin with their characteristic composition of a range of distinctive basement-clast lithology types derived from the Uncompahgre Uplift, are confined solely to the Fisher Basin; no clasts of Uncompahgre affinity are present in the succession in the other mini-basins. This demonstrates that uplift of the Fisher Valley salt wall resulted in the development of a surface topographic expression at this time that was effective in acting as a barrier to fluvial flow, thereby serving to limit the supply of sediment within the Parriott and Big Bend basins to detritus being shed from the San Luis Uplift in the southeast (Cadigan & Stewart, 1971; Stewart *et al.*, 1972).

In the Parriott Basin, the Ali Baba Member is characterised mainly by sheet-like heterolithic elements (F3) with the middle part of the member consisting of a series of vertically and horizontally amalgamated channel elements (Figs 11b, 12b). A similar arrangement of architectural elements is also present in the Big Bend Basin on the southwest flank of the Castle Valley salt wall, above the intraformational unconformity. The overall change in the style of accumulated elements between the Tenderfoot and Ali Baba members could reflect a change in climate from relatively arid to more humid conditions,

resulting in increased channelised fluvial activity, and the absence of evaporitic deposits.

### **Sewemup Member**

The preserved succession of the Sewemup Member in all three mini-basins is represented predominantly by sheet-like heterolithic elements (Fhiss; F3), with only scarce, isolated single-storey channel elements (F2) present throughout the member. The presence of gypsum-clast-bearing horizons (FGc/m) indicates that the relative rate of uplift of the Castle Valley salt wall exceeded the rate at which the adjacent basins were being infilled, resulting in the salt wall breaching the land surface such that gypsum detritus was shed into the adjacent basins and locally reworked by fluvial processes (Figs 12c, 13c; Lawton & Buck, 2006). The absence of major channel elements and the preservation of relatively soluble gypsum clasts indicate increased climatic aridity relative to that which prevailed at the time of Ali Baba Member deposition. The absence of gypsum clasts around the vicinity of the Fisher Valley salt wall and their complete absence from the Fisher Basin demonstrate that this salt wall did not breach the surface during Moenkopi deposition (Figs 11c, 12c). The sheet-like heterolithic elements (F3) represent the preserved deposits of ephemeral, non-confined floods, which swept across the basin floor (Tunbridge, 1981; Marriott *et al.*, 2005), locally reworking gypsum-clast debris.

The Sewemup Member records an upward decrease in the abundance of sand-filled channel elements (F2) and an associated systematic increase in the occurrence of sheet-like heterolithic elements (F3), which could reflect the preserved expression of a temporal reduction in sediment supply rate (Stewart *et al.*, 1972) or a shift to more arid climatic conditions.

### **Parriott Member**

During the final stages of accumulation of the Moenkopi Formation in the Salt Anticline Region, the incidence of channelised fluvial sedimentation once again increased in the Parriott and Big Bend basins relative to that indicated by deposits of the Sewemup Member. This is expressed as an increase in the occurrence of single-storey channel elements (F2) in the Parriott Basin and

multi-storey channel elements (F1) in the Big Bend Basin. The Parriott Member is absent from the preserved succession in the Fisher Basin, where the disconformity at the base of the Chinle Formation incises into the top of the Sewemup Member throughout the basin. This suggests that little or no sedimentation occurred during Parriott Member accumulation in the Fisher Basin, which likely indicates the ultimate exhaustion of the sediment derived from the Uncompahgre Uplift (Fig. 11d) and the lack of an effective sediment delivery pathway from a southerly source into the Fisher Basin. In the Parriott and Big Bend mini-basins, accumulation of the Parriott Member was mostly confined to rim synclines that had developed along both margins of the Castle Valley salt wall. The fill of the rim syncline on the Parriott Basin side of this salt wall is characterised by non-confined sheet-like (F3) elements intercalated with single-storey, multi-lateral channelised (F2) elements (Fig. 12d). The fill on the Big Bend Basin side of the Castle Valley salt wall, is significantly more sand prone, containing a series of multi-storey, multi-lateral channel elements, which are confined solely to the rim syncline directly adjacent to the uplifting salt wall (Fig. 13b, d), where enhanced accommodation was locally generated by preferential salt evacuation directly adjacent to the salt wall.

### ***Discussion***

The balance between the relative rates of sediment accumulation and basin infilling, and basin subsidence and associated salt-wall uplift is controlled by a number of factors, some of which are inherently linked to other processes involved in the development of the salt-walled mini-basins (Fig. 14). The rate of generation of accommodation within evolving mini-basins is ultimately dictated by the mechanical properties of the salt, including its initial composition and its anisotropic stratification (Hite, 1962), and the rate at which the salt can flow, which in turn depends on dynamic variables such as changes in rate at which sediment accumulates in an overlying mini-basin (Gee & Gawthorpe, 2006; Matthews *et al.*, 2007), and changes in groundwater levels and geothermal gradient. An increase in the rate of sediment loading acts to accelerate the rate of basin subsidence (Stewart & Clarke, 1999; Matthews *et al.*, 2007). Similarly, an increase in the geothermal gradient

and the presence of meteoric water both act to decrease viscosity, resulting in faster rates of salt movement (Carter & Heard, 1970; Jackson & Talbot, 1986; Davison *et al.*, 1996b). Other, fixed variables that control mini-basin evolution include initial salt thickness, style and type of stratification in salt-prone units, the location of and offset across basement faults, pre-salt basement geometries, and inherited pre-existing basin-fill state, each of which combine to exert a series of direct and indirect controls on the style of mini-basin evolution, the generation of accommodation, the orientation and spacing of salt-walls, and local anomalies in rates of salt movement within salt bodies (Hudec *et al.*, 2009, Fuchs *et al.*, 2011). The inertia of a buoyant, rising salt wall can also dictate the style and timing of both the generation of surface topography and surface breaching of the salt wall itself, which can then serve as a local sediment source; momentum forces dictate that an already rising salt wall will continue to rise even after it has attained a buoyancy equilibrium with the surrounding strata (Hudec *et al.*, 2009). The interplay between the parameters that govern salt kinematics can induce positive feedback cycles, which can in turn dictate rates and styles of sediment accumulation within parts of evolving basins, or sediment bypass (via diversion of sediment systems) in other parts. Increased rates of sediment supply and sedimentation generate increased loading and favour accelerated rates of salt withdrawal. This in turn can increase the rate of sediment capture within an individual basin, thereby driving the entire process of sediment accumulation and differential loading at a faster rate via a positive feedback mechanism. This process can occur within an individual basin where differential rates of subsidence occur at different points in the same mini-basin, resulting in locally increased or decreased rates of salt withdrawal and accommodation generation. Associated increased rates of salt-wall uplift might be expressed in the sedimentary record as the increased presence of intraformational clasts (Fci), derived locally from the reworking of strata eroded from above the uplifting salt walls. In cases where the salt walls breach the surface, reworked clasts of salt would be expected, especially in cases where an arid climatic regime prevents dissolution.

The thickness of salt through which the mini-basins subsided throughout their development defines the maximum potential depth of a mini-basin and the total potential accommodation. The configuration of the Paradox Basin allowed the accumulation of thicker deposits of salt of the Paradox Formation in the foredeep area where the thickest accumulations of sediment are accommodated within the salt-walled mini-basins of the Salt Anticline Region (Kluth & DuChene, 2009; Trudgill & Paz, 2009; Trudgill 2011). Prior to the onset of sedimentation of the Moenkopi Formation, the basin-fill state of the studied mini-basins, in terms of the extent to which accommodation was filled by fluvial, shallow-marine and aeolian strata of the Honaker Trail Formation and Undifferentiated Cutler Group, drove the main phase of mini-basin subsidence and infilling. This defined the geometry of the basins at the time of accumulation of the Moenkopi Formation.

In the Fisher basin, the pre-Triassic basin-fill is the thickest of any mini-basin in the Salt Anticline Region and this basin was apparently already close to grounding on sub-salt basement by the onset of Moenkopi deposition (Trudgill & Paz, 2009). This resulted in slow subsidence rates throughout the episode of accumulation of the Moenkopi Formation in the Fisher basin and, coupled with relatively higher rates of sediment delivery and accumulation during deposition of the Ali Baba Member, accommodation in the Fisher basin was rapidly filled by a sand-prone interval composed of a complex of multi-storey channel elements (F1). Toward the end of the episode of accumulation of the Sewemup Member, rates of delivery of sand-grade sediment to the Fisher basin slowed dramatically as the sediment source area of the Uncompahgre Uplift was denuded, resulting in the accumulation of a sand-poor interval composed of sheet-like heterolithic elements (F3).

The Parriott basin was filled to a lesser degree by pre-Triassic sediment (Trudgill & Paz, 2009; Trudgill, 2011), meaning there was significant inherited accommodation available for filling during deposition of the Moenkopi Formation. This, combined with a higher rate of ongoing subsidence than that experienced by the Fisher Basin, resulted in the accumulation of a thicker succession of Moenkopi Formation in the Parriott basin. The rate of sediment

delivery to the Parriott basin was low relative to that of the Fisher basin and major channel complexes did not develop, resulting in the accumulation of a thick but generally sand-poor succession, with minor sand-prone intervals present only in the Ali Baba and Parriott Members, the latter arising from the preferential diversion of channels into a developing rim syncline.

The rate of generation of accommodation and its rate of filling by accumulating fluvial systems can be explained in terms of a series of Barrell diagrams (Barrell, 1917) for different areas within each mini-basin (Fig. 15). In locations where rates of subsidence outpaced rates of sediment delivery, the accumulating stratigraphy became dominated by a relatively argillaceous succession (Fig. 15; log 3) of heterolithic sheet-like elements (F3). In locations where rates of subsidence and sedimentation were balanced, sand-prone successions tended to accumulate (Fig. 15; log 1) and multi-storey multi-lateral channel elements (F1) and single-storey multi-lateral channel elements (F2) dominated the succession. In locations where rates of sedimentation outpaced rates of subsidence, erosion and sediment by-pass ensued and stacked multi-storey, multi-lateral channel elements (F1) containing abundant intraformational conglomerate (Fci) lags accumulated (Fig. 15; log 5) as fluvial systems repeatedly reworked older deposits as they migrated across the filled basin floor. Locations that experienced uplift, such as salt-wall flanks, experienced localised bypass and/or erosion and intraformational unconformities developed as a result of later fluvial incision (Fig. 15; log 7).

## **Conclusions**

1. The Moenkopi Formation demonstrates that the preserved expression of fluvial systems in salt-walled mini-basins is directly controlled by: (i) the distribution of available accommodation (i.e. space yet to be filled) inherited from earlier basin-fill episodes, as demonstrated by the spatial variations of stratigraphic thickness both between and within mini-basins; (ii) the prevailing climate and rate and pathway of sediment delivery, which dictate fluvial processes and the pattern and distribution of architectural elements between and within mini-basins; (iii) the rate of ongoing salt-

induced subsidence beneath evolving mini-basins and that rate of uplift of bounding salt walls, which together dictate the rate of generation of additional accommodation.

2. Sediment within individual mini-basins accumulated contemporaneously throughout the duration of Moenkopi Formation deposition, as demonstrated by the similar characteristic features of each of the members present across all three studied mini-basins.
3. Pre-existing basin-fill architectures inherited from the pre-Triassic sediment-fill state of the mini-basins exerted a significant control on subsequent subsidence during accumulation of the Moenkopi Formation. The Fisher basin (closest to the Uncompahgre Uplift) underwent greater subsidence and sediment filling during the Permian than the Parriott and Big Bend mini-basins, mainly a result of the direction of sediment delivery. The megafan responsible for the accumulation of the undifferentiated Cutler Group delivered sediment across the salt walls, such that the Fisher basin became preferentially filled and subsided to a point close to grounding on the pre-salt strata early in its history. As a consequence, the Moenkopi Formation in the Fisher basin is relatively thin, the succession experienced only slow rates of subsidence and sediment accumulation. Higher rates of mini-basin subsidence and accumulation of strata of the Moenkopi Formation characterised the basins further away from the Uncompahgre Uplift.
4. Subsurface salt-wall growth acted to uplift overlying strata to generate a surface topography, the growth of which was effective in diverting fluvial drainage pathways, especially in areas where salt-wall uplift culminated in surface breaching by the growing salt wall. During deposition of the Moenkopi Formation, preferred fluvial flow pathways were aligned parallel to the trend of the elongate salt walls, which served to effectively partition neighbouring mini-basins. Where salt walls breached the surface (e.g. Castle Valley salt wall), gypsum detritus was shed as clasts into the surrounding mini-basins and locally reworked by fluvial processes before being preserved in the basin-fill.
5. The point-of-entry of a major fluvial drainage system into a subsiding mini-basin and its preferred flow pathway within the basin dictate the rate and

style of accumulation. This is recorded in the preserved fluvial succession whereby fairways of major fluvial activity are preserved as single-storey or multi-storey, multi-lateral channel elements.

6. Salt-wall uplift served to isolate fluvial systems and confine them within their respective mini-basins. As a result of this confinement and isolation, each fluvial system within a specific mini-basin could theoretically be supplied from a different source area. As a result, the preserved expression of the fluvial architecture generated by each isolated fluvial system might vary considerably between adjacent mini-basins. In the Moenkopi Formation, this is expressed as the accumulation of relatively sand-poor intervals at the same stratigraphic levels as relatively sand-prone intervals in adjacent basins. Examples in the Salt Anticline Region include: (i) the difference in sand content between the Ali Baba Member in the Parriott basin versus the Fisher basin; and (ii) the difference in sediment architecture between the Parriott Member in the Parriott and Big Bend basins.
7. Spatial variations in both mini-basin subsidence rate and sedimentation delivery rate act as primary controls on fluvial system accumulation style. Packages of sand-prone strata can be preserved in one part of a mini basin at apparently the same stratigraphic level as packages of sand-poor strata elsewhere in the same mini-basin (e.g. northeast side versus the southwest side of the Parriott Basin).

### ***Acknowledgements***

This research was funded by Areva, BHP Billiton, ConocoPhillips, Nexen, Saudi Aramco, Shell and Woodside through their sponsorship of the Fluvial & Eolian Research Group at the University of Leeds. Layla Cartwright is thanked for field assistance. Jo Venus, Tom Heron, Tom Reynolds, Stuart Clarke, Ian Kane and Bill McCaffrey provided valuable field discussions. We are grateful to reviewers David Barbeau and Timothy Lawton and to Editor Brian Horton for their constructive advice and comments.

### ***References***

ALA, M.A. (1974) Salt Diapirism in Southern Iran. *Am. Assoc. Petrol. Bull.*, **58**, 1758-1770.

AL-ZOUBI, A. & TEN BRINK, U.S. (2001) Salt diapirs in the Dead Sea basin and their relationship to Quaternary extensional tectonics. *Mar. and Petrol. Geol.*, **19**, 779-797.

ANDRIE, J.R., GILES, K.A., LAWTON, T.F. & ROWAN, M.G. (2012) Halokinetic-sequence stratigraphy, fluvial sedimentology, and structural geometry of the Eocene Carroza Formation along La Popa salt weld, La Popa Basin, Mexico. In: *Salt Tectonics, Sediments, and Prospectivity* (Ed. by I.G. Aslop, S.G. Archer, A.J. Hartley, N.T. Grant & R. Hodgkinson). Spec. Publ. Geol. Soc. London. , **363**, 59-79.

ASCHOFF, J.L. & GILES, K.A. (2005) Salt diapir-influenced shallow-marine sediment dispersal patterns: Insights from outcrop analogs. *Am. Assoc. Petrol. Geol. Bull.*, **89**, 447-469.

BAARS, D.L. (1966) Pre-Pennsylvanian paleotectonics – key to basin evolution and petroleum occurrences in Paradox basin, Utah and Colorado. *Am. Assoc. Petrol. Geol. Bull.*, **50**, 2082-2111.

BAKER, A.A., DOBBIN, C.E., MCKNIGHT, E.T. & REESIDE, J.B. (1927) Notes on the Stratigraphy of the Moab region, Utah. *Am. Assoc. Petrol. Geol. Bull.*, **11**, 785-808.

BARBEAU, D.L. (2003) A flexural model for the Paradox basin: implications for the tectonics of the Ancestral Rocky Mountains. *Basin Res.*, **15**, 97-115.

BARDE, J-P., CHAMBERLAIN, P., GALAVAZI, M., GRALLA, P., HARWIJANTO, J., MARSKY, J. & VAN DEN BELT, F. (2002) Sedimentation during halokinesis: Permo-Triassic reservoirs of the Saigak Field, Precaspian Basin, Kazakhstan. *Petrol. Geosci.*, **8**, 177-187.

BARREL, J. (1917) Rhythms and the Measurement of Geologic Time. *Bull. Geol. Soc. Am.*, **28**, 745-904.

BARTON, D.C. (1933) Mechanics of formation of salt domes with specific reference to Gulf Coast salt domes of Texas and Louisiana. *Am. Assoc. Petrol. Geol. Bull.*, **17**, 1025-1083.

BLAKEY, R.C. (1973) Stratigraphy and origin of the Moenkopi Formation (Triassic) of southeastern Utah. *The Mountain Geologist*. **10**, 1-17.

BLAKEY, R.C. (1974) Stratigraphy and Depositional Analysis of the Moenkopi Formation, Southeastern Utah. *Utah Geological and Mineral Survey Bulletin* **104**.

BLAKEY, R.C. & RANNEY, W. (2008) *Ancient Landscapes of the Colorado Plateau*. Grand Canyon Association, Grand Canyon, Arizona.

BLAKEY, R.C. (2009) Palaeogeography and geologic history of the western ancestral rocky mountain, Pennsylvanian-Permian, southern Rocky Mountains and Colorado Plateau In: *The Paradox Basin Revisited – New Developments in Petroleum Systems and Basin Analysis* (Ed. by W.S. Houston, L.L. Wray, & P.G. Moreland), pp. 222-264. Rocky Mountain Association of Geologists, Denver, CO.

CAIN, S.A. & MOUNTNEY, N.P (2009) Spatial and temporal evolution of a terminal fluvial fan system: the Permian Organ Rock Formation, South-east Utah, USA. *Sedimentology*, **56**, 1774-1800.

CAIN, S.A. & MOUNTNEY, N.P. (2011) Downstream changes and associated fluvial-aeolian interactions in an ancient terminal fluvial fan system: the Permian Organ Rock Formation, SE Utah. In: *From River to Rock Record* (Ed. by S. Davidson, S. Leleu, and C .North), SEPM Spec. Publ., **97**, 165-187.

CARTER, N.L. & HEARD, H.C. (1970) Temperature and rate dependent deformation of halite. *Am. J. Sci.*, **269**, 193-249.

CATER, F.W. (1970) Geology of the Salt Anticline Region in Southwestern Colorado. Department of the Interior, United States Geological Survey Bulletin, **637**.

CADIGAN, R.A. & STEWART, J.H. (1971) Petrology of the Triassic Moenkopi Formation and Related Strata in the Colorado Plateau Region. Department of the Interior, United States Geological Survey Professional Paper **692**.

DANE, C.H. (1935) Geology of the Salt Valley anticline and adjacent areas Grand County, Utah. Department of the Interior, United States Geological Survey Bulletin, **863**.

CONDON, S.M (1997) Geology of the Pennsylvanian and Permian Cutler Group and Permian Kaibab Limestone in the Paradox Basin, Southeastern Utah and Southwest Colorado. *Department of the Interior, U.S. Geological Survey Bulletin 2000-P*

DARTON, N.H. (1910) A reconnaissance of parts of northwestern New Mexico and northern Arizona. Department of the Interior, United States Geological Survey Bulletin, **435**.

DAVISON, I., BOSENCE, D., ALSOP, I.G. & AL-AWAH, M.H. (1996a) Deformation and sedimentation around active Miocene salt diapirs on the Tihama Plain, northwest Yemen. In: *Salt Tectonics* (Ed. by I.G. Alsop, D.J. Blundell & I. Davison), Spec. Publ.Geol. Soc. London, **100**, 23-39.

DAVISON, I., ALSOP, I.G. & BLUNDELL, D. (1996b) Salt tectonics: some aspects of deformation mechanics. In: *Salt Tectonics* (Ed. by I.G. Alsop, D.J. Blundell & I. Davison), Spec. Publ.Geol. Soc. London, **100**, 1-10.

DOELLING, H.H. (1988) Geology of salt valley anticline and Arches National Park, Grand County, Utah. In: *Salt Deformation in the Paradox Region* (Ed. by H.H. Doelling, C.G. Oviatt & P.W. Huntoon), *Utah Geol. Surv. Bull.*, **122**, 7-58.

DOELLING, H.H. (2002a) *Geologic Map of the Fisher Towers 7.5' Quadrangle, Grand County, Utah*. Utah Geol. Surv. Geologic Map 183, p.22.

DOELLING, H.H. (2002b) Geological map of the Moab and eastern parts of the San Rafael Desert 30' x 60' quadrangles Grand and Emery Counties, Utah and Mesa County, Colorado. Utah Geol. Surv. Geologic Map 180.

ELISTON, D.P., SHOEMAKER, E.M. & LANDIS, E.R. (1962) Uncompahgre front and salt anticline region of the Paradox Basin, Colorado and Utah. *Am. Assoc. Petrol. Geol. Bull.*, **46**, 1857-1878.

FIDUK, J.C. (1995) Influence of submarine canyon erosion and sedimentation on allochthonous salt body geometry: the pathway of Bryant Canyon in Garden Banks. In: *Salt, Sedimentation, and Hydrocarbons* (Ed. by C.J. Travis, B.C. Vendeville, H. Harrison, F.J. Peel, M.R. Hudec & B.E. Perkins). GCSSEPM Foundation 16<sup>th</sup> Annual Research Conference, 41-51.

FRIEDMAN, J.D., CASE, J.E. & SIMPSON, S.L. (1994) Tectonic Trends of the Northern Part of the Paradox Basin, Southeastern Utah and Southwestern Colorado, As Derived From Landsat Multispectral Scanner Imaging and Geophysical and Geologic Mapping. *U.S. Department of the Interior, U.S. Geological Survey Bulletin*, **2000-C**.

FUCHS, L., SCHMELING, H. & KOYI, H. (2011) Numerical models of salt diapir formation by downbuilding: the role of sedimentation rate, viscosity contrast and initial amplitude and wavelength. *Geophys. J. Int.*, **186**, 390-400.

GEE, M.J.R. & GAWTHORPE R.L. (2006) Submarine channels controlled by salt tectonics: Examples from 3D seismic data offshore Angola. *Mar. Petrol. Geol.*, **23**, 443-458.

GE H., JACKSON, M.P.A. & VENDEVILLE B.C. (1997) Kinematics and Dynamics of Salt Tectonics Driven by Progradation. *Am. Assoc. Petrol. Geol. Bull.*, **81**, 398-423.

GOODALL, T.M., NORTH, C.P. & GLENNIE, K.W. (2000) Surface and subsurface sedimentary structures produced by salt crusts. *Sedimentology*, **47**, 99-118.

GOLDHAMMER, R.K., OSWALD, E.J., & DUNN, P.A. (1991) Hierarchy of stratigraphic forcing: Examples from the Middle Pennsylvanian self carbonates of the Paradox basin. *Kansas Geol. Surv. Bull.*, **233**, 361-413.

GREGORY, H.E. (1917) Geology of the Navajo Country: A reconnaissance of parts of Arizona, New Mexico, and Utah. Department of the Interior United States Geological Survey Professional Paper **93**.

HALL, D.J. & THIES, K.J. (1995) Salt kinematics, depositional systems, and implications for hydrocarbon exploration, Eugene Island and Ship Shoal south additions, offshore Louisiana. In: *Salt, Sedimentation, and Hydrocarbons* (Ed. by C.J. Travis, B.C. Vendeville, H. Harrison, F.J. Peel, M.R. Hudec & B.E. Perkins). GCSSEPM Foundation 16<sup>th</sup> Annual Research Conference, 83-94.

HARRISON, T.S. (1927) Colorado-Utah salt domes. *Am. Assoc. Petrol. Geol. Bull.*, **11**, 111-113.

HINDS, D.J., ALIYEVA, E., ALLEN, M.B., DAVIES, C.E., KROONENBERG, S.B., SIMMONS, M.D., VINCENT, S.J. (2004) Sedimentation in a discharge dominated fluvial-lacustrine system: the Neogene productive series of the South Caspian Basin, Azerbaijan. *Mar. Petrol. Geol.*, **21**, 613-638.

HINTZE, L.F. & AXEN, G.J. (1995) Geology of the Lime Mountain Quadrangle, Lincoln Country, Nevada. Nevada Bureau of Mines and Geology Map 129.

HITE, R.J. (1968) Salt Deposits of the Paradox Basin, Southeast Utah and Southwest Colorado. In: *Saline Deposits – A Symposium based on Papers from the International Conference on Saline Deposits, Houston, Texas, 1962*. (Ed. by: R.B. Mattox, W.T. Holser, H. Ode, W.L. McIntyre, N.M. Short, R.E. Taylor & D.C. Van Sicken) *Geol. Soc. Am. Spec. Pap.*, **88**, 319-330.

HODGSON, N.A., FARNSWORTH, J. & FRASER, A.J. (1992) Salt-related tectonics, sedimentation and hydrocarbon plays in the Central Graben, North Sea, UKCS. In: *Exploration Britain: Geological insights for the next decade* (Ed. by R.F.P. Hardman), *Spec. Publ. Geol. Soc. London*, **67**, 31-63.

HUDEC, M.R. (1995) The Onion Creek salt diapir: an exposed diapir fall structure in the Paradox Basin, Utah. In: *Salt, Sedimentation, and Hydrocarbons* (Ed. by C.J. Travis, B.C. Vendeville, H. Harrison, F.J. Peel, M.R. Hudec & B.E. Perkins). GCSSEPM Foundation 16<sup>th</sup> Annual Research Conference, 125-134.

HUDEC, M.R. & JACKSON, M.P.A. (2007) Terra infirma: Understanding salt tectonics. *Earth Sci. Rev.*, **82**, 1-28.

HUDEC, M.R., JACKSON, M.P.A. & SCHULTZ-ELA, D.D. (2009) The Paradox of minibasin subsidence into salt: Clues to the evolution of crustal basins. *Geol. Soc. Am. Bull.*, **121**, 201-221.

INGS, S.J. & BEAUMONT, C. (2010) Shortening viscous pressure ridges, a solution to the enigma of initiating salt 'withdrawal' minibasins. *Geology*, **38**, 339-342.

JACKSON, M.P.A. & TALBOT, C.J. (1986) External shapes, strain rates, and dynamics of salt structures. *Geol. Soc. Am. Bull.*, **97**, 305-323.

JACKSON, M.P.A., CORNELIUS, R.R., CRAIG, C.H., GANSSER, A., STOCKLIN, J. & TALBOT, C.J. (1990) Salt diapirs of the Great Kavir, Central Iran. *Geol. Soc. Am. Mem.* **177**.

JACKSON, M.P.A., VENDEVILLE, B.C. & SCHULTZ-ELA, D.D. (1994) Structural dynamics of salt systems. *Annu. Rev. Earth Planet. Sci.* **22**, 93-117.

JONES, R.W. (1959) Origin of Salt Anticlines of the Paradox Basin. *Am. Assoc. Petrol. Geol. Bull.*, **43**, 1869-1895.

JONES, A.D., AULD, H.A., CARPENTER, T.J., FETKOVICH, E., PALMER, I.A., RIGATOS, E.N. & THOMPSON, M.W. (2005) Jade Field: and innovative approach to high-pressure, high temperature field development. *Petroleum Geology Conference series 2005*, **6**, 269-283.

JORDAN, O.D. & MOUNTNEY, N.P. (2010) Styles of interaction between aeolian, fluvial and shallow marine environments in the Pennsylvanian-Permian Lower Cutler Beds, southeast Utah, USA. *Sedimentology*, **57**, 1357-1385.

JORDAN, O.D. & MOUNTNEY, N.P. (2012) Sequence stratigraphic evolution and cyclicity of an ancient coastal desert system: the Pennsylvanian-Permian lower Cutler beds, Paradox Basin, Utah, USA. *J. Sediment. Res.*, **82**, 755-780.

KERNEN, R.A., GILES, K.A., ROWAN, M.G., LAWTON, T.F. & HEARON, T.E. (2012) Depositional and halokinetic-sequence stratigraphy of the Neoproterozoic Wonoka Formation adjacent to Patawarta allochthonous salt sheet, Central Flinders Ranges, South Australia. In: *Salt Tectonics, Sediments, and Prospectivity* (Ed. by I.G. Aslop, S.G. Archer, A.J. Hartley, N.T. Grant & R. Hodgkinson). Spec. Publ. Geol. Soc. London, **363**, 81-105.

KLUTH, C.F. & CONEY, P.J. (1981) Plate tectonics of the Ancestral Rocky Mountains. *Geology*, **9**, 10-15.

KLUTH, C.F. & DU CHENE, H.R. (2009) Late Pennsylvanian and early Permian structural geology and tectonic history of the Paradox Basin and Uncompahgre uplift, Colorado and Utah. In: *The Paradox Basin Revisited – New Developments in Petroleum Systems and Basin Analysis* (Ed. by W.S. Houston, L.L. Wray, & P.G. Moreland), pp. 178-197. Rocky Mountain Association of Geologists, Denver, CO.

LAWTON, T.F. & BUCK, B.J. (2006) Implications of diapir-derived detritus and gypsic palaeosols in Lower Triassic strata near the Castle Valley salt wall, Paradox Basin, Utah. *Geology*, **34**, 885-888.

LINDHOLM, R. (1987) *A practical approach to Sedimentology*, 1<sup>st</sup> Ed.. Allen & Unwin, Inc, Massachusetts.

MACK, G. H. & RASMUSSEN, K.A. (1984) Alluvial-Fan Sedimentation of the Cutler Formation (Permo-Pennsylvanian) Near Gateway, Colorado. *Geol. Soc. Am. Bull.*, **95**, 109-116.

MATTHEWS, W.J., HAMPSON, G.J., TRUDGILL, B.D. & UNDERHILL, J.R. (2007) Controls on fluvio-lacustrine reservoir distribution and architecture in passive salt diapir provinces: insights from outcrop analogue. *Am. Assoc. Petrol. Geol. Bull.*, **91**, 1367-1403.

MATTOX, R.B. (1968) Salt Anticline Field Area, Paradox Basin, Colorado and Utah. In: *Saline Deposits – A Symposium based on Papers from the International Conference on Saline Deposits, Houston, Texas, 1962*. (Ed. by: R.B. Mattox, W.T. Holser, H. Ode, W.L. McIntyre, N.M. Short, R.E. Taylor & D.C. Van Sicken) *Geol. Soc. Am. Spec. Pap.*, **88**, 5-16.

MCKIE, T. & AUDRETSCH, P. (2005) Depositional and structural controls on Triassic reservoir performance in the Heron Cluster, ETAP, Central North Sea. In: *North-West Europe and Global Perspectives – Proceedings of the 6<sup>th</sup> Petroleum Geology Conference*, 285-297

MARRIOTT, S.B., WRIGHT, V.P. & WILLIAMS, B.P.J (2005) A new evaluation of fining upward sequences in a mud-rock dominated succession of the Lower Old Red Sandstone of South Wales, UK. *Fluvial sedimentology VII, Int. Assoc. Sedimentol. Spec. Publ.*, **35**, 517-529.

MIALL, A.D (1985) Architectural-Element Analysis: A New Method of Facies Analysis Applied to Fluvial Deposits. *Earth Sci. Rev.*, **22**, 261-308.

MIALL, A.D. (1996) *The Geology of Fluvial Deposits*. Springer, Berlin.

MORALES, M. (1987) Terrestrial Fauna and Flora from the Triassic Moenkopi Formation of the Southwestern United States. *J. Arizona-Nevada Acad. Sci.*, **22**, 1-19.

NEWBERRY, J.S. (1861) Geological Report. In Ives, J.C., Report upon the Colorado River of the West: U.S. 36th Cong. 1st Sess. *Senate and House Ex. Doc*, **90**, pt. 3, 154.

NEWELL, A.J., BENTON, M.J., KEARSEY, T., TAYLOR, G., TWITCHETT, R.J. & TVERDOKHLEBOV, V.P. (2012) Calcretes, fluviolacustrine sediments and subsidence patterns in Permo-Triassic salt-walled minibasins of the south Urals, Russia. *Sedimentology*, **59**, 1659-1676.

OHLEN, H.R. & MCINTYRE, L.B. (1965) Stratigraphy and tectonic features of the Paradox Basin, four corners area. *Am. Assoc. Petrol. Geol. Bull.*, **49**, 2020-2040.

PAZ, M., TRUDGILL, B. & KLUTH, C. (2009) Salt System Evolution of the Northern Paradox Basin. *Search and Discovery Article #30078*.

PROCHNOW, S.J., ATCHLEY, S.C., BOUCHER, T.E., NORDT, L.C. & HUDEC, M.R. (2006) The influence of salt withdrawal subsidence on palaeosol maturity and

cyclic fluvial deposition in the Upper Triassic Chinle Formation: Castle Valley, Utah. *Sedimentology*, **53**, 1319-1345.

PRATHER, B.E. (2009) Calibration and visualization of depositional process models for above-grade slopes: a case study from the Gulf of Mexico. *Mar. Petrol. Geol.*, **17**, 619-638.

RASMUSSEN, L. & RASMUSSEN, D.L. (2009) Burial history analysis of the Pennsylvanian petroleum system in the deep Paradox Basin fold and fault belt, Colorado and Utah. In: *The Paradox Basin Revisited – New Developments in Petroleum Systems and Basin Analysis* (Ed. by W.S. Houston, L.L. Wray, & P.G. Moreland), pp. 24-94. Rocky Mountain Association of Geologists, Denver, CO.

SELLY, R.C. (1988) *Applied Sedimentology*. Academic Press Limited, London.

SHOEMAKER, E.M. (1955) Structural features of the central Colorado Plateau and their relation to uranium deposits. In: *Contributions to the Geology of Uranium and Thorium by the United States Geological Survey and Atomic Energy Commission for the United Nations Commission for the United Nations International Conference on Peaceful Uses of Atomic Energy, Geneva, Switzerland*. Department of the Interior, Geological Survey Professional Paper 300.

SHOEMAKER, E.M. & NEWMAN, W.L. (1957) Notes on the Moenkopi Formation in the Salt Anticline Region of Colorado and Utah. U.S. Department of the Interior, U.S. Geological Survey Trace Elements Investigations Report **681**.

SHOEMAKER, E.M. & NEWMAN, W.L. (1959) Moenkopi formation (Triassic? and Triassic) in Salt Anticline Region, Colorado and Utah. *Am. Assoc. Petrol. Geol. Bull.*, **42**, 1835-1851.

SLOSS, L.L. (1969) Evaporite Deposition from Layered Solutions. *Am. Assoc. Petrol. Geol. Bull.* **53**, 776-789.

SMITH, R.I., HODGSON, N., & FULTON, M. (1993) Salt control on Triassic reservoir distribution, UKCS Central North Sea. In: *Petroleum Geology of Northwest Europe: Proceedings of the 4<sup>th</sup> Conference* (Ed. by J.R. Parker) pp.547-557. Geol. Soc. London.

STEWART, J.H. (1959) Stratigraphic relations of Hoskinnini Member (Triassic?) of Moenkopi Formation on Colorado Plateau. *Am. Assoc. Petrol. Geol. Bull.* **43**, 1852-1868.

STEWART, J.H., POOLE, F.G. & WILSON, R.F., CADIGAN, R.A. (1972) Stratigraphy and origin of the Triassic Moenkopi Formation and related strata in the Colorado Plateau region. US Department of the Interior, US Geological Survey Professional Paper, **691**.

STEWART, S.A. (2007) Salt tectonics in the North Sea Basin: a structural style template for seismic interpreters. In: *Deformation of the Continental Crust: The Legacy of Mike Coward* (Ed. by A.C. Ries, R.W.H. Butler, R.H. Graham), *Spec. Publ. Geol. Soc. London*, **272**, 361-396.

STEWART, S.A. & CLARKE, J.A. (1999) Impact of salt on the structure of the Central North Sea hydrocarbon fairways. *Petroleum Geology Conference series*, **5**, 179-200.

TALBOT, C.J. (1998) Extrusion of Hormuz salt in Iran. In: *Lyell: the past is the Key to the Present*. (Ed. by D.J. Blundell, & A.C. Scott), *Spec. Publ. Geol. Soc. London*, **143**, 315-334.

TALBOT, C.J. & AFTABI, P. (2004) Geology and models of salt extrusion at Qum Kuh, central Iran. *J. Geol. Soc. London*. **161**, 321-334.

TRUDGILL, B.D (2011) Evolution of salt structure in the northern Paradox Basin: controls on evaporite deposition, salt wall growth and supra-salt stratigraphic architecture. *Basin Res.*, **23**, 208-238.

TRUDGILL, B., BANBURY, N. & UNDERHILL, J. (2004) Salt-evolution as a control on structural and stratigraphic systems: northern Paradox foreland basin, SE Utah, USA. In: *Salt-Sediment Interactions and Hydrocarbon Prospectively: Concepts, Applications and Case Studies for the 21<sup>st</sup> Century*. Gulf Coast State Society of Economic Paleontologists and Mineralogists Foundation, 24<sup>th</sup> Bob F. Perkins Research Conference Proceedings (CD-ROM) (Ed. by P.J. Post) pp. 132-177. Gulf Coast Section SEPM Foundation, Huston, Texas.

TRUDGILL B.D & PAZ, M. (2009) Restoration of mountain front and salt structures in the Northern Paradox Basin, S.E. Utah. *The Paradox Basin Revisited – New Developments in Petroleum Systems and Basin Analysis* (Ed. by W.S. Houston, L.L. Wray, & P.G. Moreland), pp. 132-177. Rocky Mountain Association of Geologists, Denver, CO.

TRUSHEIM, F. (1960) Mechanisms of salt migration in northern Germany. *Am. Assoc. Petrol. Geol. Bull.* **9**, 1519-1540

TUNBRIDGE, I.P. (1981) Old Red Sandstone Sedimentation – An example from the Brownstones (highest Lower Old Red Sandstone) of South Central Wales. *Geol. J.*, **16**, 111-124.

VENDEVILLE, B.C. & JACKSON, M.P.A. (1992a) The fall of diapirs during thin-skinned extension. *Mar. Petrol. Geol.*, **9**, 354-371.

VENDEVILLE, B.C. & JACKSON, M.P.A. (1992b) The rise of diapirs during thin-skinned extension. *Mar. Petrol. Geol.*, **9**, 331- 353

VENUS, J.H., MOUNTNEY, N.P., & MCCAFFREY, W.D. [In Review] Synsedimentary salt diapirism as a control on fluvial system evolution: an example from the Permian Cutler Group, SE Utah, U.S.A. *Basin Res.*

VOLOZH, Y., TALBOT, C., & ISMAILI-ZADEH, A. (2003) Salt structures and hydrocarbons in the Pricaspian basin. *Am. Assoc. Petrol. Geol. Bull.*, **87**, 313-334.

WALTHAM, D. (1997) Why does salt start to move? *Tectonophysics*, **282**, 117-128.

WARD, L.F. (1901) Geology of the Little Colorado Valley. *Am. J. Sci.* **12**, 401-413.

WILLIAMS, M.R. (1996) Stratigraphy of Upper Pennsylvanian Cyclical Carbonate and Siliciclastic Rocks, Western Paradox Basin, Utah. In: *Paleozoic systems of the Rocky Mountain Region* (Ed. by M.W. Longman & M.D. Sonnenfield) Rocky Mountain Section, SEPM, 283-304.

WILLIAMS, M.R. (2009) Stratigraphy of Upper Pennsylvanian cyclic carbonate and siliciclastic rocks, western Paradox Basin, Utah. In: *The Paradox Basin Revisited – New Developments in Petroleum Systems and Basin Analysis* (Ed. by W.S. Houston, L.L. Wray, & P.G. Moreland), pp. 381-435, Rocky Mountain Association of Geologists, Denver, CO.

WILLIAMS-STROUD, S. (1994) The evolution of an inland sea of marine origin to a non-marine saline lake: the Pennsylvanian Paradox salt. In: *Sedimentology and Geochemistry of Modern and Ancient Saline Lakes* (Ed by R.W. Renaut & W.M. Last), SEPM Spec. Publ., **50**, 293-306.

WU, S., BALLY, A.W. & CRAMEZ, C. (1990) Allochthonous salt, structure and stratigraphy of the north-eastern Gulf of Mexico. Part II: Structure. *Mar. Petrol. Geol.*, **7**, 334-370.

## **Figure and Table Captions**

**Table 1.** Lithofacies recorded in the Salt Anticline Region study area. Abbreviations: Ang = Angular; SA = Sub-angular; SR = Sub-rounded; Mod. = moderate sorting; M.Fine = medium- to fine-grained sandstone.

**Fig. 1.** Regional map of the Paradox Basin and associated Uncompahgre and San Luis uplifts. Map depicts the limits of the Paradox Basin based on the extent of subsurface salt deposits of the Paradox Formation, and the depositional limit of the Moenkopi Formation (modified in part from Barbeau, 2003; Condon, 1997; Shoemaker & Newman, 1959; Stewart *et al.*, 1972).

**Fig. 2.** Overview map of the Salt Anticline Region and study area. Map depicts the location of measured sedimentary sections, and lines of correlation panels. Map centre: 38.70°N, 109.324°W; geodetic system: WGS 84.

**Fig. 3.** Regional stratigraphic column and palaeocurrent summary data. Column depicts the average thickness of the various stratigraphic units in the Salt Anticline Region, and average thicknesses of Moenkopi Formation and its constituent members within the individual studied mini-basins. Palaeocurrent summary data for each mini-basin are plotted as rose diagrams for which vector mean, vector magnitude, and number of recorded readings are shown. Regional stratigraphic column after Trudgill (2011).

**Fig. 4.** Representative measured sections from the 3 studied mini-basins: Parriott basin section is from Parriott Mesa South East; Fisher basin section is from Fisher Valley Mega; Big Bend basin section is from Big Bend Campsite C.

**Fig. 5.** Representative lithofacies of the Moenkopi Formation in the Salt Anticline Region. See Table 1 for explanation of lithofacies codes. (a) Trough cross-bedded sandstone (Fxt) with intraformational clasts (Fci). 1: Underlying erosive base. 2: Medium- to coarse- grained trough cross-bedded sandstone facies with a high proportion of intraformational clasts. 3: Clasts are angular to sub-rounded. (b) Fluvial channel filled with intraformational clasts (Fci). 1: Channel incised into underlying HA Fxp facies. 2: Fluvial channel filled with orthoconglomerate; pebble-grade clasts of intraformational origin (Fci). Matrix is medium- to coarse-grained sandstone. 3: Cross-bedded sandstone set of medium-grained sandstone with isolated pebble-grade clasts of intraformational origin. (c) Trough cross-bedded sandstone (Fxt). 1: Larger-scale cross-bedding is indicative of larger bedforms developed in main channels. 2: Thin foresets within troughs. 3: Intersecting trough cut-offs in sections perpendicular to flow generated by the migration of sinuous-crested dunes with out-of-phase successive bedform crestlines. (d) Horizontally laminated sandstone (Fh). 1: Horizontally laminated sands composed of fine-

grained sandstone exhibit thinner laminations than in examples composed of coarse-grained sandstone. 2: Colour mottling and reduction associated with slightly less permeable layers. (e) Climbing ripple strata (Frc). 1: Subcritical climbing ripple stratification in sets composed of fine- to medium-grained sandstone. 2: Positive but subcritical angle-of-climb. 3: Palaeoflow direction. (f) Wave-ripple laminated sandstone (WR). 1: Ripple forms preserved on upper bedding surface seen in section and exhibiting a combination of chevron-style accumulation and draping of foresets onto ripple-crests. 2: Some examples of asymmetric ripples indicate mixed unidirectional and bidirectional flow regime typical of sluggish flow in shallow water influenced by surface wind shear. (g) Gypsum-clast-bearing unit; matrix supported (FGm). 1: Gypsum clasts are sub-angular: indicative of short transport distance. 2: Matrix-supported nature of sets indicates deposition by debris flow or water flow. 3: Pebble-grade clast horizon overlain by coarse-grained granulestone of gypsum micro-conglomerate, indicating disaggregation of larger clasts in higher energy flows, or possibly indicative of longer transport distances. (h) Horizontal interbedded sandstones and siltstones (Fhiss). 1: Subcritical climbing ripple strata in fine-grained sandstone. 2: Thin beds of climbing ripple strata are interbedded with thin sets of siltstone. 3: Palaeoflow direction.

**Fig. 6.** Representative architectural elements of the Moenkopi Formation, detailing the most common meso-scale elements present in the Salt Anticline Region.

**Fig. 7.** Photomontages of macro-scale basin-fill architectural styles. (a) Aerial photograph of the Red Hills (also known as the “Truck and Boat” structure) at the northwest tip of the Castle Valley salt wall. The nature of the uplift is asymmetric, with the western salt-wall flank characterised by a slope geometry and the eastern salt-wall flank characterised by a ramp-flat-ramp trajectory. Note the intraformational unconformity on the west flank of the uplift. (b) Photograph and interpretation panel of the western salt-wall flank slope geometry. Abundance of channel sand-body occurrence decreases upslope toward the crest of the salt wall. The succession thins by 25 m between the two logs, which are situated 270 m apart. High resolution photographs of

growth strata depicted in the inserts are available in the on-line supplementary material.

**Fig. 8.** Correlation panels depicting spatial changes in thickness of members of the Moenkopi Formation and the internal distribution of distinctive architectural features. See Fig. 2 for location of panels. Sewemup Member is divided into gypsum-bearing facies and non-gypsum-bearing facies. (a) Correlation panel for the Parriott basin depicting the thinning of the Moenkopi Formation towards the tip of the Castle Valley salt wall. (b) Correlation panel for the Fisher basin depicting near-constant thickness of the members. Note, however, the significant relief on the disconformity at the base of the overlying Chinle Formation. (c) Correlation panel across all 3 studied mini-basins. Note the asymmetric style of the basin profile in the Parriott basin, and the absence of the Parriott Member from the Fisher basin. Additional material depicting a more detailed view of the architectural relationships of the members adjacent to the Castle Valley salt wall is available in the on-line supplementary material.

**Fig. 9.** (a) Model for Salt Anticline Region depicting deposition of the Ali Baba Member. (b) Detailed stratigraphic model for the Parriott basin. (c & d) Examples of fluvial architectural elements F1 & F3, which are two of the main elements composing the majority of the basin fill.

**Fig. 10.** Model to account for the temporal evolution of the Fisher basin. The preserved stratigraphic architecture demonstrates a slow initial episode of subsidence prior to eventual cessation of subsidence prior to accumulation of the Parriott Member. The upper part of the Moenkopi Formation (above the Ali Baba Member) records a gradual reduction in the abundance of elements indicative of sedimentation via channelised fluvial processes in the basin.

**Fig. 11.** Model to account for the temporal evolution of the Parriott basin. The preserved stratigraphic architecture demonstrates asymmetric subsidence within the basin, with higher rates of subsidence occurring on the margin of the Castle Valley salt wall. During accumulation of the Sewemup Member, the

Castle Valley salt wall breached the land surface and acted as a source of gypsum-clast detritus.

**Fig. 12.** Model to account for the temporal evolution of the Big Bend basin. The only fully exposed section of the Moenkopi Formation in the Big Bend basin was exposed on the flank of the Castle Valley salt wall where 245 m of Moenkopi Formation is exposed. In the central part of the basin, only the upper part of the Sewemup Member and the Parriott Member are exposed.

**Fig. 13.** Conceptual diagram depicting the interaction of the main parameters that either directly or indirectly affect rates of sedimentation, basin subsidence and salt-wall uplift. See text for explanation.

**Fig. 14.** Model depicting the effects of differential rates of subsidence and accommodation generation on basin-fill style in a salt-walled mini-basin. Barrell diagrams to show basin subsidence rates and sedimentation rates for various locations in an evolving mini-basin. In areas where rates of sedimentation and subsidence are balanced, sand-prone successions tend to accumulate, whereas where rates of subsidence outpace rates of sediment delivery, heterolithic, sand-poor successions tend to accumulate and basins remain partly unfilled. Note that changes in sediment type and supply rates can result in complex changes in sedimentary architecture.

Code	Facies	Colour	Grain size & Texture	Composition	Primary Sed. Structures	Secondary Sed. Structures	Interpretation
<b>Fm</b>	Massive	Orange-brown	V.Fine to V.Coarse. Ang to SR	Quartzo-feldspathic sand	Some graded bedding	Rarely colour reduced	Rapid deposition from suspension
<b>Fxt</b>	Trough cross-bedding	Purple-brown to orange-brown	Medium to Coarse. Mod. Sorting, SA-SR	Quartzo-feldspathic sand	Trough cross-bedding		Downstream migration of sinuous-crested dune-scale mesoforms
<b>HA Fxp</b>	High-angle planar cross-bedding	Purple-brown to orange-brown	Medium to Coarse. Mod. Sorting, SA-SR	Quartzo-feldspathic sand	Trough cross-bedding		Straight-crested or sinuous-crested dunes migrating within a fluvial channel (can be trough cross-bedding rotated through 90 degrees)
<b>LA Fxp</b>	Low-angle planar cross-bedding	Purple-brown to orange-brown	M.Fine to Coarse. Mod. Sorting SA-SR	Quartzo-feldspathic sand	Low-angle planar cross-bedding		Migration of lateral accretion mesoforms
<b>Fxl/Frc</b>	Cross laminated / climbing ripple strata	Orange-brown to red-brown	V.Fine to Medium. Mod. Sorting, SA - SR	Quartzo-feldspathic sand	Current ripple lamination: sub- to super-critical climb	Rarely colour reduced	Unidirectional migration of microforms within channels or unconfined flows under low flow regime. Fxl is the preserved expression of sinuous-crested climbing ripples. Frc may be sinuous- or straight-crested.
<b>Fh</b>	Horizontally laminated	Orange-brown, red-brown or red-grey	V.Fine to Fine. Mod - Well sorting, SA-SR	Quartzo-feldspathic sand	Primary current lamination; normal grading	Rarely colour reduced	Deposition from upper-flow regime, either from channel flow or from non-confined sheet flow
<b>Fci</b>	Intraformational clasts	Dark-brown clasts; light-brown matrix	5mm to 70mm clasts, Fine to Medium matrix	Mudstone clasts and sandstone	Weak imbrication		Represents erosion and re-deposition of locally reworked sediments in channel-belt and floodplain areas
<b>Fce</b>	Extraformational clasts	Green, purple, reds & white	5mm to 70mm clasts, Fine to Medium matrix	Basement lithologies	Weak imbrication if matrix supported		Represents transportation of basement clasts into the depositional environment, possibly by a high-energy flood event
<b>FGm</b>	Gypsum clasts; matrix supported	White clasts with orange or chocolate-brown	10mm to 150mm clasts, Fine to Medium matrix	Gypsum and sand matrix			Generated during episodes of salt-wall breaching at surface. Represents slow rates of salt delivery in areas proximal to salt wall, or location distal from salt wall
<b>FGc</b>	Gypsum clasts; clast supported	White clasts with minor amount of orange matrix	10mm to 150mm clasts, Fine to Medium matrix	> 80% gypsum clasts.	Weak imbrication		Generated during episodes of salt-wall breaching at surface. High rates of delivery of salt clasts in areas proximal to the salt wall
<b>Gc</b>	Crystalline gypsum bed	White to grey	Crystalline	>95% gypsum	May display inclined or horizontal lamination		Clinofolds generated by gypsum aeolian dune form migration (Lawton & Buck, 2006)
<b>Gb</b>	Gypsum-bound sandstone	Orange-Brown to "Cutler purple"-brown	Usually Fine to Medium. Poor sorting, Angular	Gypsum cement	Usually massive bedding	Gypsum cementation	Origin possibly by post-depositional throughflow of dissolved gypsum resulting in cementation
<b>Fd</b>	Deformed bedding	Orange-brown to chocolate-brown	V.Fine to Med. grain. Mod to Poor, SA-SR	Quartzo-feldspathic sand	Horizontal lamination; current-ripple lamination	Load & flame; dewatering; slumps	Soft-sediment deformation resulting from loading of unconsolidated sediments and associated water-escape. Slumps may indicate movement of sediment down slope, syn or post deposition
<b>Scls</b>	Crinkly Laminated sandstones	Orange sst.	Fine to Med. Sandstone SA-SR	Quartzo-feldspathic sand, and silt	Crinkly laminations: laminations are discordant		Represents disruption of sedimentary structures by ground water movement by capillary action (Goodall <i>et al.</i> , 2000)
<b>WR</b>	Wave ripple strata	Orange to chocolate-brown or grey	V.Fine to M.Fine sandstone.	Quartzo-feldspathic sand	Symmetrical ripple forms	Typically reduced	Represents bi-directional flow created by surface waves on shallow-water ponds on the alluvial plain
<b>Fhiss</b>	Horizontally interbedded silts and sands	Orange sst., with chocolate brown silt	Fine to Coarse sst., and silt. Poor sorting	Quartzo-feldspathic sand, and silt	Can contain Facies <b>WR, Fm, Frc/Fxl, Fh, rare Fci</b>	desiccation cracks infilled with Fm.	Represents multiple flood events where progressively finer material is deposited with corresponding sedimentary structures from a waning flow.

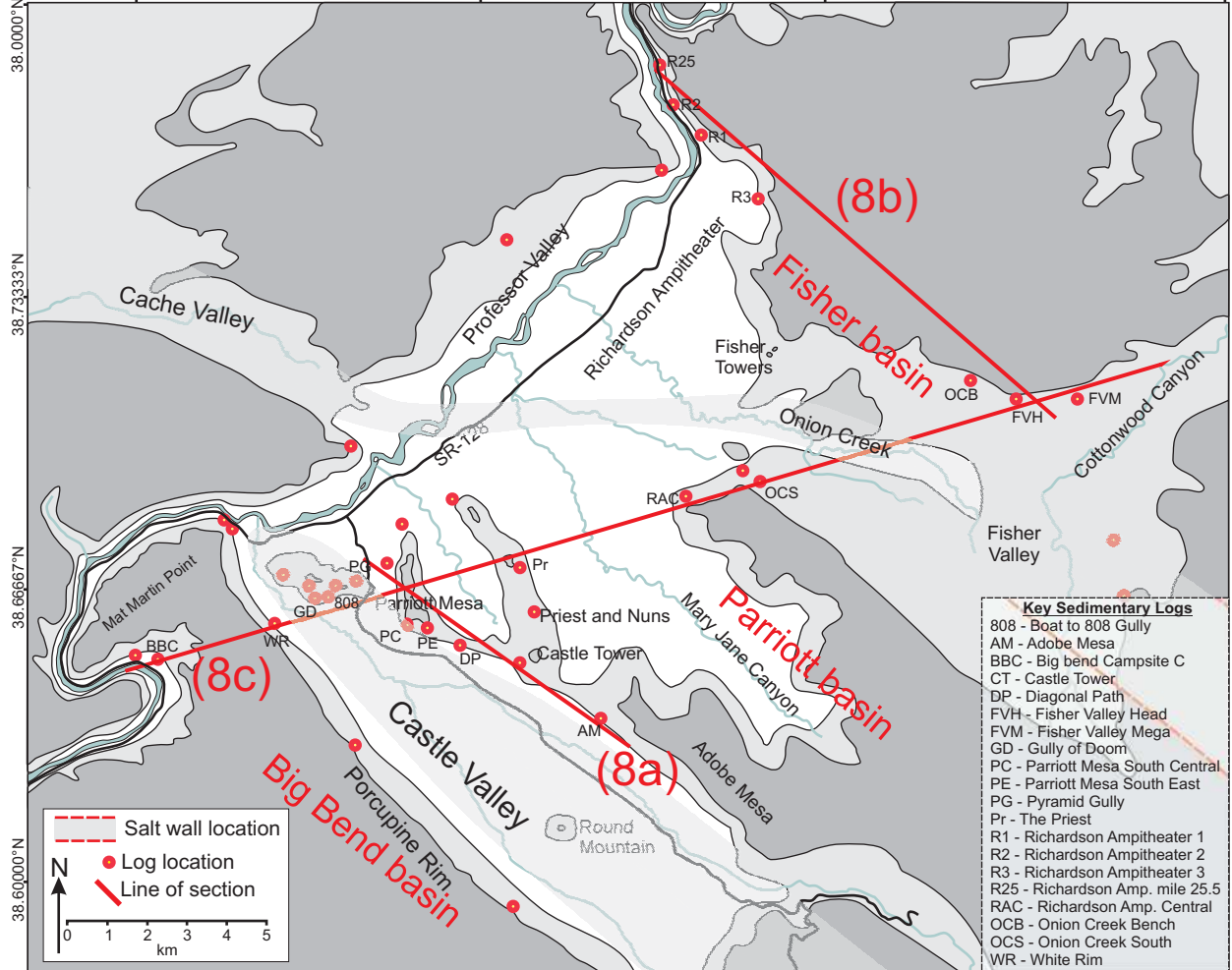


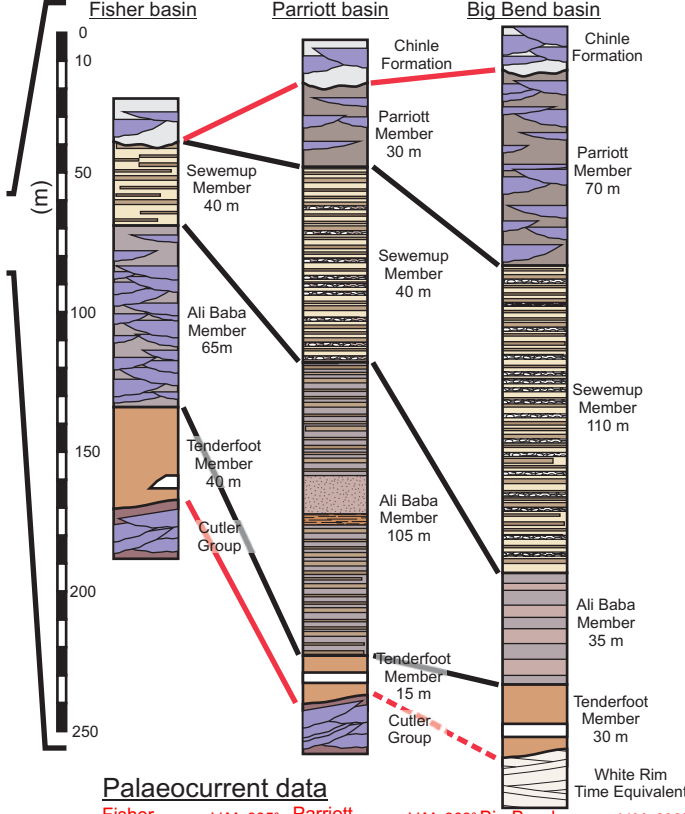
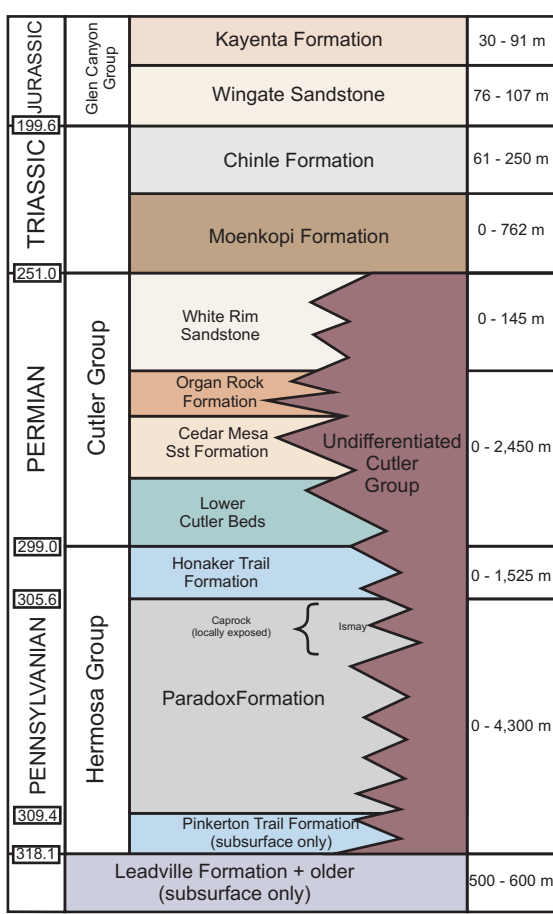
109.48333°W

109.38333°W

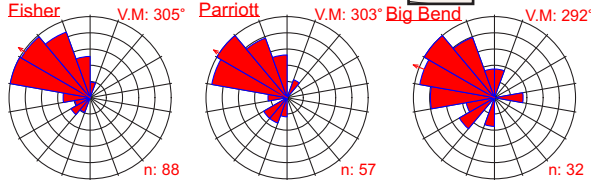
109.28333°W

109.16667°W



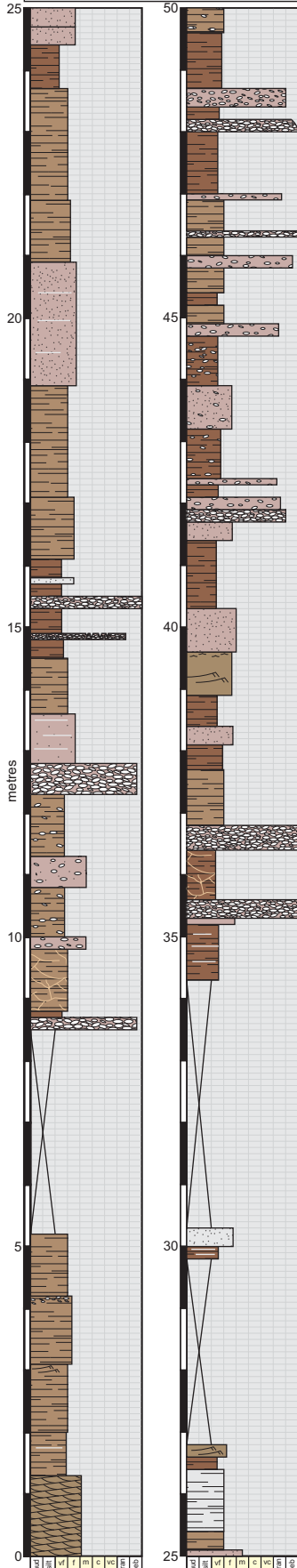


**Palaeocurrent data**



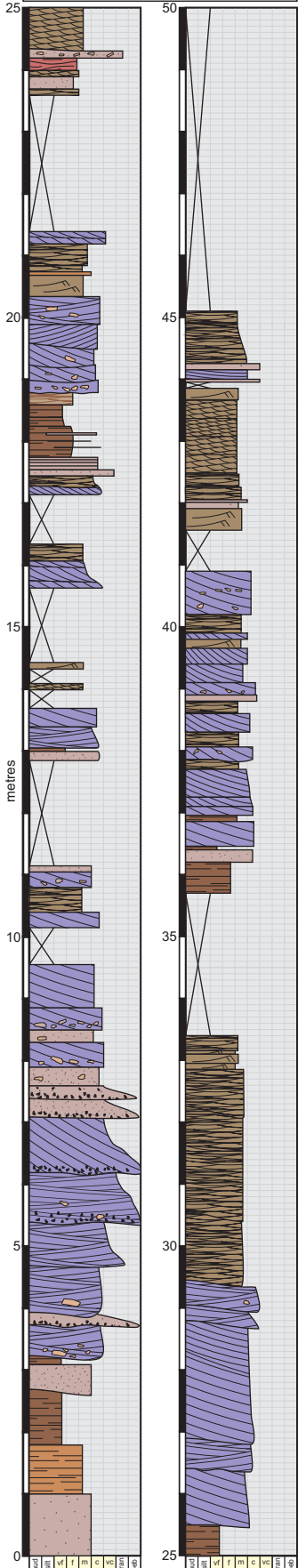
**Parriott basin - Parriott Mesa South East**

Total Log Thickness: 210m  
 Co-ordinates:  
 12 S 0638642 / 4279751  
 Elevation at base: 1418m



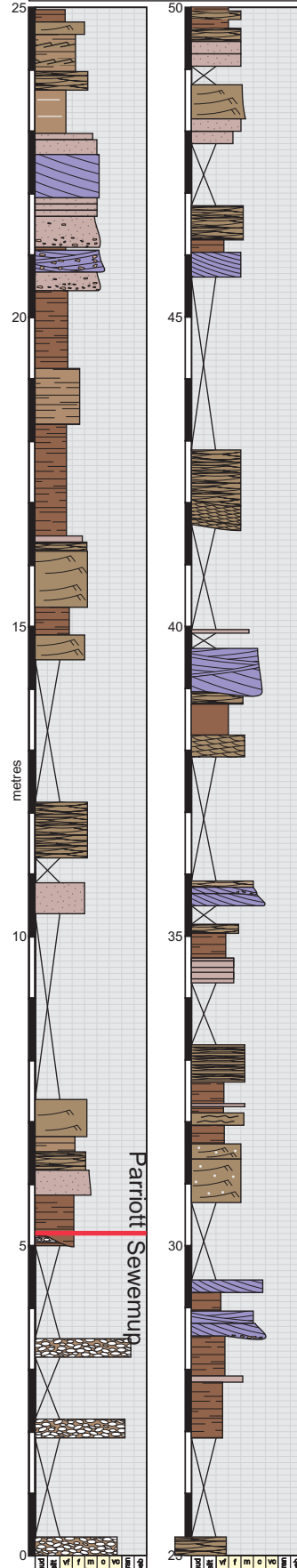
**Fisher basin - Fisher Valley Mega**

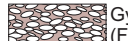
Log Thickness: 108 m  
 Co-ordinates:  
 12 S 0655666 / 4286123  
 Elevation at base: 1781 m



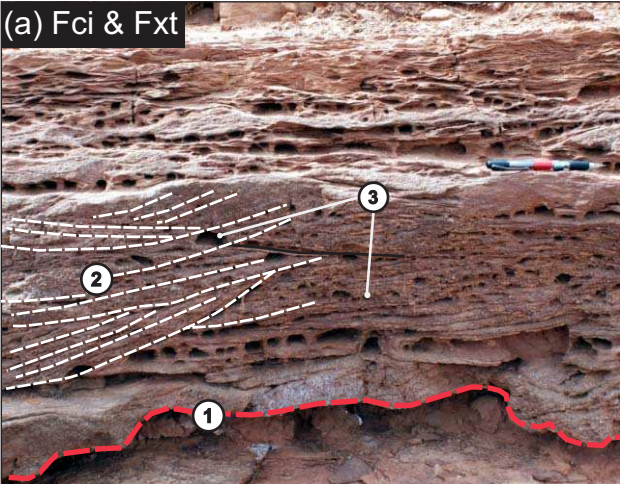
**Big Bend basin - Big Bend Campsite C**

Log Thickness: 75 m  
 Co-ordinates:  
 12 S 631964 / 4279163  
 Elevation at base: 1228 m

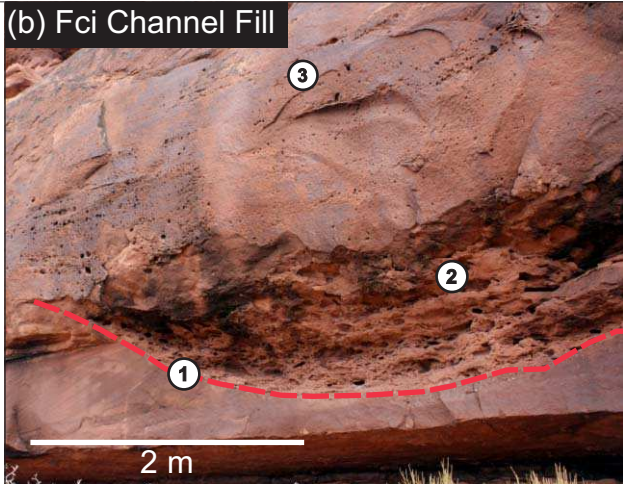


- |  |   |  |  |
|--|---|--|--|
|  Massive sandstone (Fm)                |  Mesoscale bedforms (Fxt, Fxp)       |  Deformed bedding (Fd)            |  Interbedded Heterolithic strata (FHiss) |
|  Horizontally laminated sandstone (Fh) |  Microscale bedforms (Frc, Fxl, Frw) |  Gypsum-clast horizons (FGm, FGc) |  Siltstone (Heterolithic strata) (Fd)    |

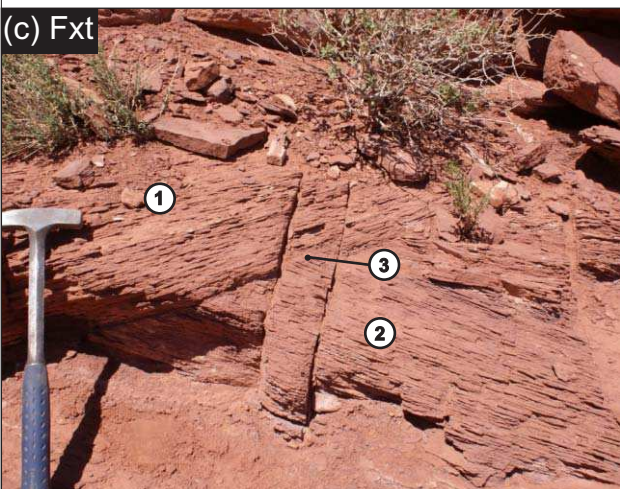
(a) Fci & Fxt



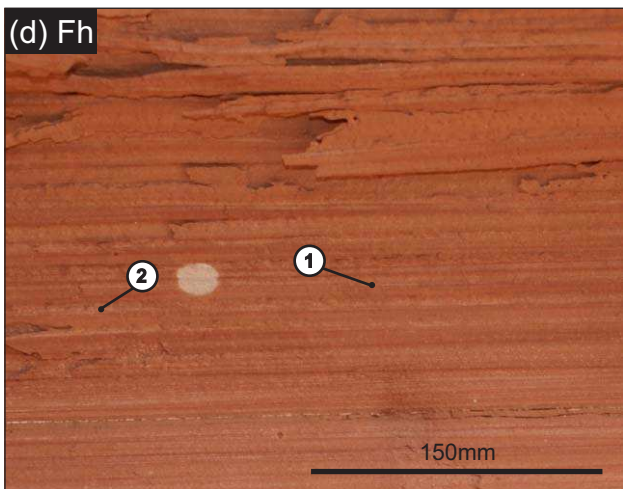
(b) Fci Channel Fill



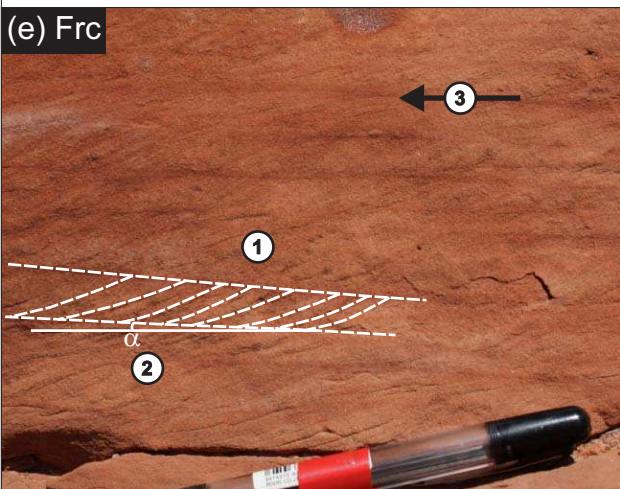
(c) Fxt



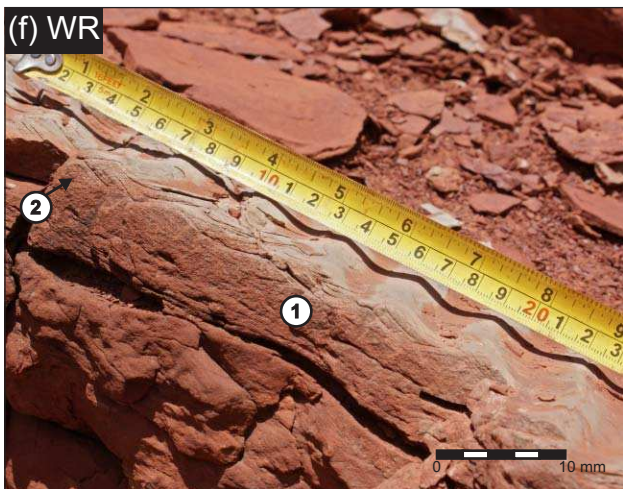
(d) Fh



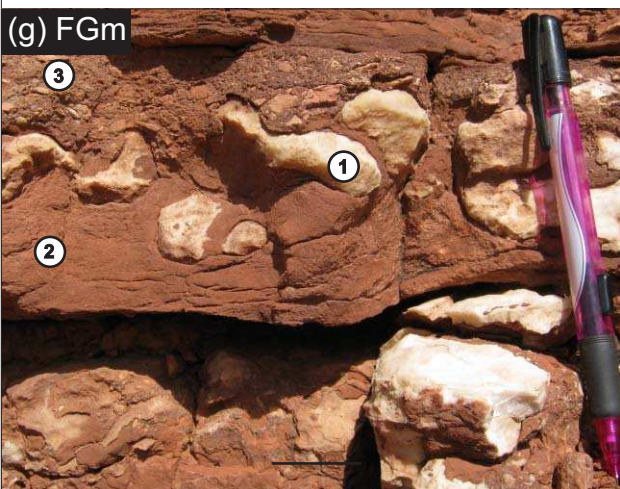
(e) Frc



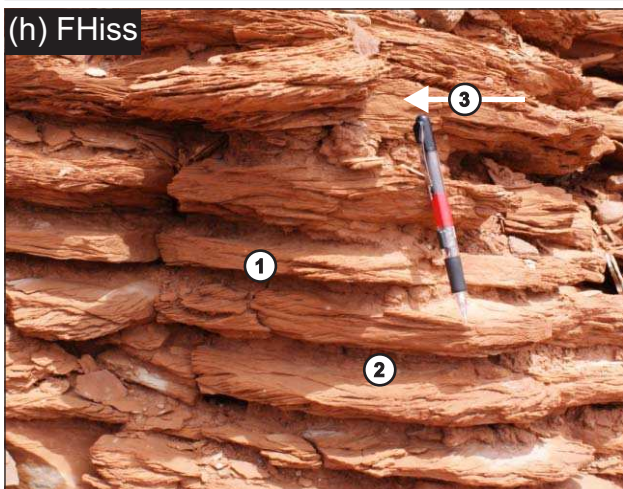
(f) WR



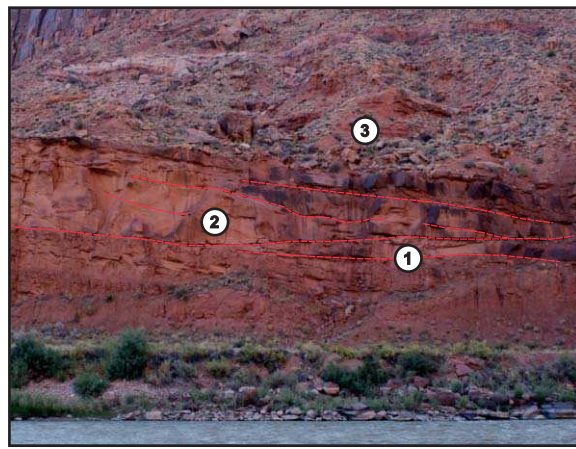
(g) FGm



(h) FHiss



# Representative Architectural Elements



## F1 - Amalgamated Channel Elements

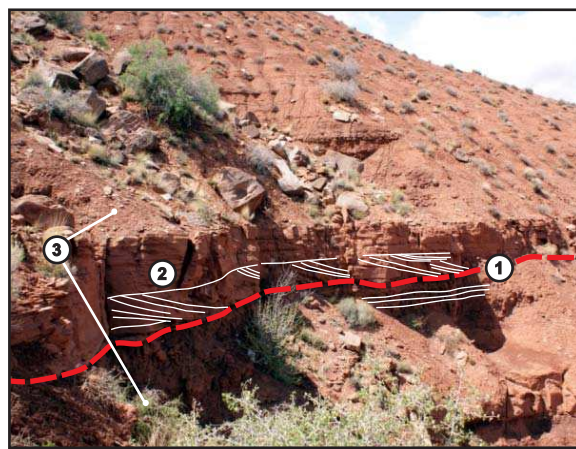
Element description	Multi-storey, multi-lateral channel elements
Element Type	Confined flow
Geometries	Multiple incised and filled channel elements
Associated Facies	Fm, Fh Fxt/Fxp, Frc/Fxl, Fce & Fci Lags
Vertical Extent	5 to 10 m
Lateral Extent	500 m to 10s km

### Key Element Characteristics

- Multiple levels of erosive undulating basal contacts.
- Channel fills are a mixture of Fm, Fxt/Fxp, and Fce & Fci Lags.
- Amalgamated channel-element complex is superceded by overbank elements.

### Interpretation

**Represents lateral accretion and vertical stacking of fluvial channel elements over time.**



## F2 - Single-Storey Channel Elements

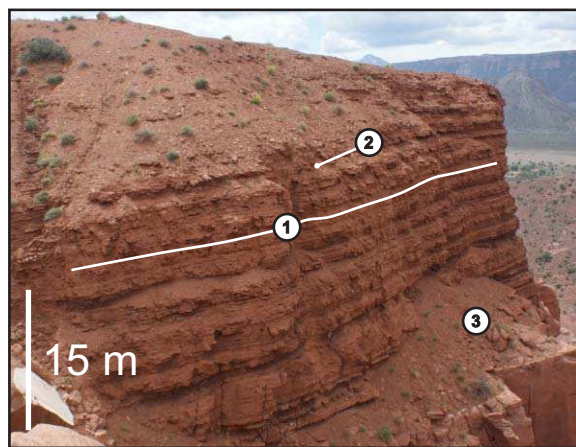
Element description	Single-storey, multi-lateral channel elements
Element Type	Confined flow
Geometries	Channel elements with no vertical stacking
Associated Facies	Fm, Fh, Fxt/Fxp, Frc/Fxl, Fce & Fci Lags
Vertical Extent	0.5 to 3 m
Lateral Extent	200 m to 10s km

### Key Element Characteristics

- Erosive undulating basal contact.
- Trough cross-bedded sandstone (Fxt), with associated climbing ripple-strata (Frc) in channel belt element.
- Element preceded and superceded by overbank sheet-flood elements (Heterolithic silts and fine sands).

### Interpretation

**Represents preserved elements created by a single channel or multiple channel migrating laterally on a single horizon.**



## F3 - Sheet-like Element (Style 1)

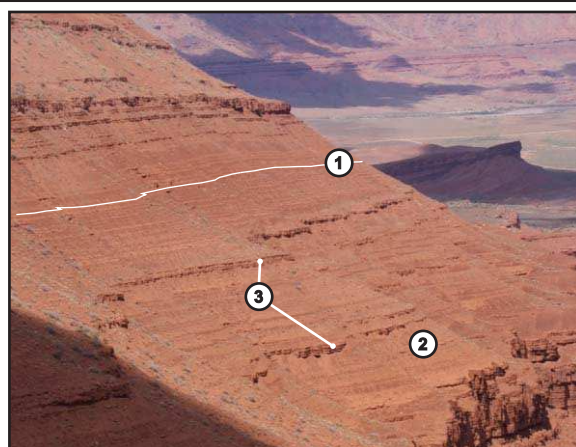
Element description	Sheet-like interbedded heterolithic silt and sandstones
Element Type	Nonconfined or unconfined flows
Geometries	Laterally extensive sheet-like bodies
Associated Facies	Fm, Fh, Frc/Fxl, Fci, desiccation cracks
Vertical Extent	0.2 m to 20 m +
Lateral Extent	500 m to several km's

### Key Element Characteristics

- Very laterally continuous - seen contouring the hill side for several km
- Can form thick monotonous successions 10s m thick.
- Friable nature of constituent facies means outcrops tend to weather to scree over any significant distance.

### Interpretation

**Represents an event where flood water was not confined within channels and sediment transport and deposition happened outside of channel elements.**



## F3 - Sheet Elements (Style 2)

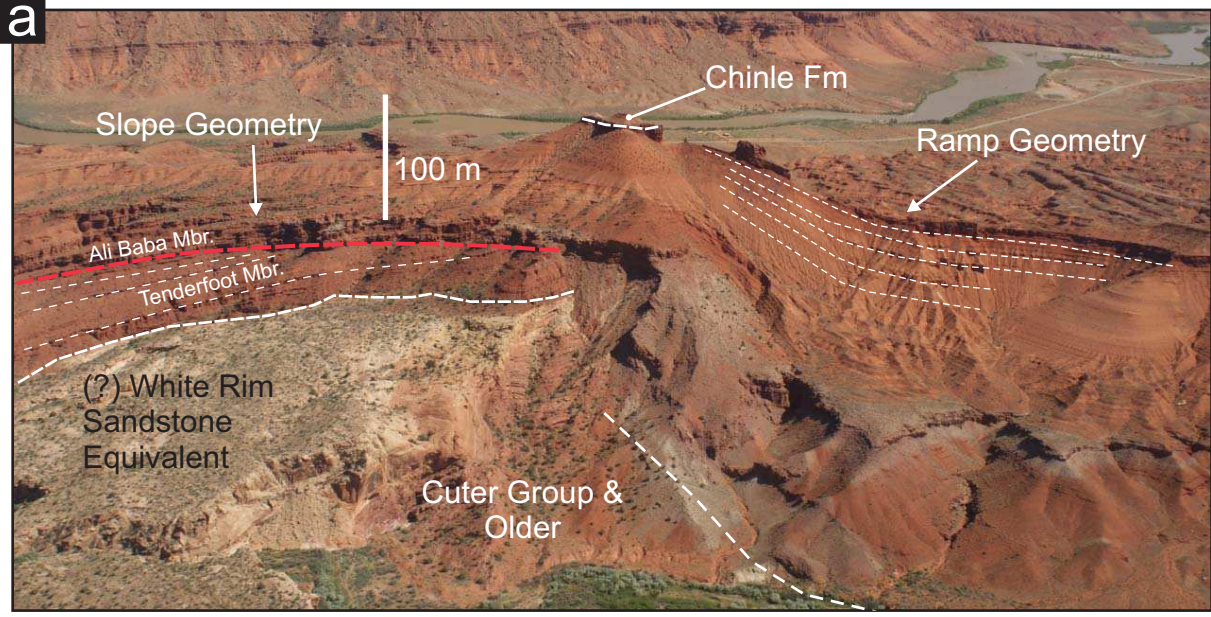
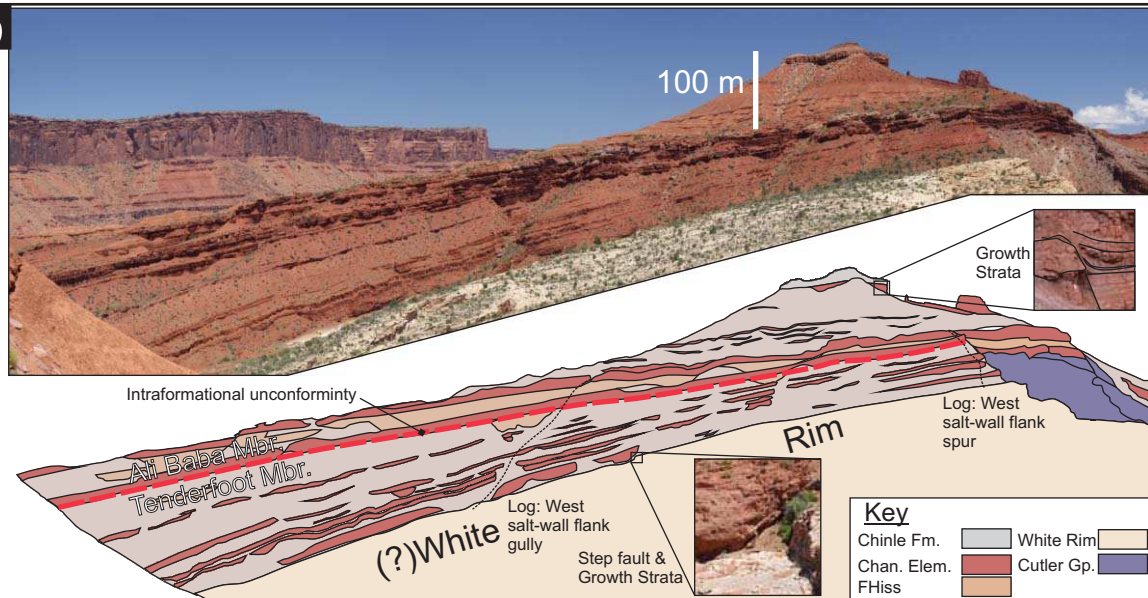
Element description	Sheet-like interbedded heterolithic silt and sandstones
Element Type	Non or unconfined flows
Geometries	Laterally extensive sheet-like bodies, can pinch out
Associated Facies	Fm, Fh, Frc/Fxl, Fci, desiccation cracks
Vertical Extent	0.2 m to 20 m +
Lateral Extent	500 m to several km's

### Key Element Characteristics

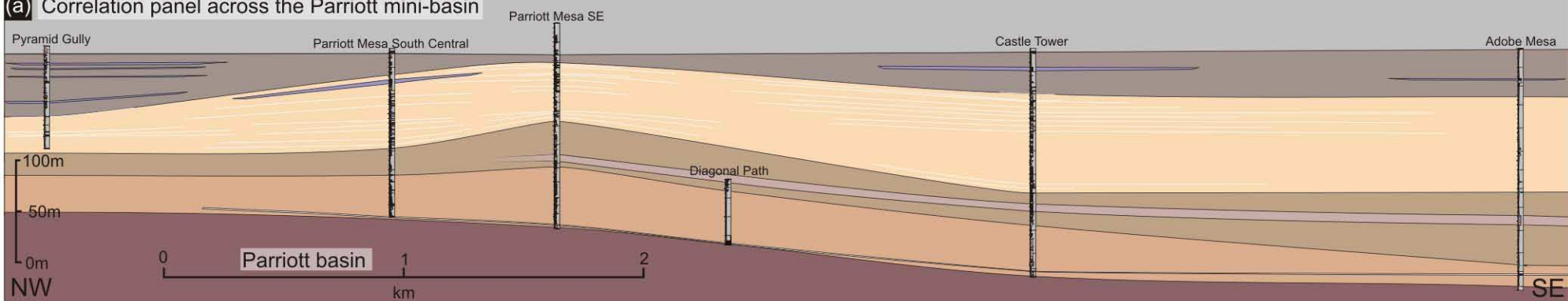
- Laterally continuous - seen contouring hill side for several km's.
- Friable nature of constituent facies means outcrops tend to weather to scree over any significant distance.
- Channel elements, which are more sand-prone weather proud.

### Interpretation

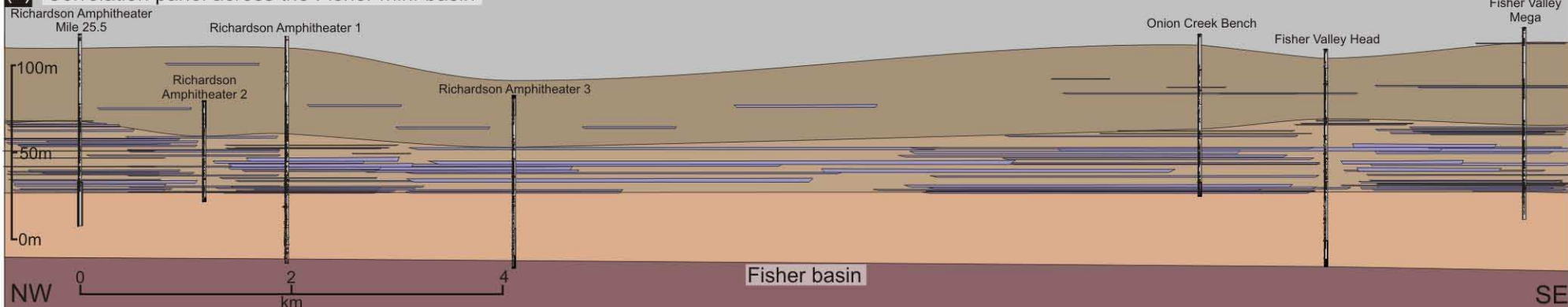
**Nature of sheet elements results in these types of elements preferentially degrading to scree, leaving channel elements as short but laterally extensive cliff sections.**

**a****b**

**(a)** Correlation panel across the Parriott mini-basin



**(b)** Correlation panel across the Fisher mini-basin



**(c)** Correlation panel of the Big Bend, Parriott and Fisher mini-basins

